

A Hierarchy of Energy- and Flux-Budget (EFB) Turbulence Closure Models for Stably-Stratified Geophysical Flows

S. S. Zilitinkevich · T. Elperin · N. Kleeorin ·
I. Rogachevskii · I. Esau

Received: 23 October 2011 / Accepted: 22 August 2012 / Published online: 13 September 2012
© Springer Science+Business Media B.V. 2012

Abstract Here we advance the physical background of the energy- and flux-budget turbulence closures based on the budget equations for the turbulent kinetic and potential energies and turbulent fluxes of momentum and buoyancy, and a new relaxation equation for the turbulent dissipation time scale. The closure is designed for stratified geophysical flows from neutral to very stable and accounts for the Earth's rotation. In accordance with modern experimental evidence, the closure implies the maintaining of turbulence by the velocity shear at any gradient Richardson number Ri , and distinguishes between the two principally different regimes: “strong turbulence” at $Ri \ll 1$ typical of boundary-layer flows and characterized by the practically constant turbulent Prandtl number Pr_T ; and “weak turbulence” at $Ri > 1$ typical of the free atmosphere or deep ocean, where Pr_T asymptotically linearly increases with increasing Ri (which implies very strong suppression of the heat transfer compared to the momentum transfer). For use in different applications, the closure is formulated at different levels of complexity, from the local algebraic model relevant to the steady-state regime

S. S. Zilitinkevich (✉)
Finnish Meteorological Institute, Helsinki, Finland
e-mail: sergej.zilitinkevich@fmi.fi

S. S. Zilitinkevich
Division of Atmospheric Sciences and Geophysics, University of Helsinki, Helsinki, Finland

S. S. Zilitinkevich · I. Esau
Nansen Environmental and Remote Sensing Centre, Bjerknes Centre for Climate Research,
Bergen, Norway

S. S. Zilitinkevich
Department of Radio Physics, N.I. Lobachevski State University of Nizhny Novgorod, Nizhny Novgorod,
Oblast, Russia

S. S. Zilitinkevich
A.M. Obukhov Institute of Atmospheric Physics, Moscow, Russia

T. Elperin · N. Kleeorin · I. Rogachevskii
Department of Mechanical Engineering, Ben-Gurion University of the Negev, Beer-Sheva, Israel

of turbulence to a hierarchy of non-local closures including simpler down-gradient models, presented in terms of the eddy viscosity and eddy conductivity, and a general non-gradient model based on prognostic equations for all the basic parameters of turbulence including turbulent fluxes.

Keywords Boundary layers · Critical Richardson number · Eddy viscosity · Conductivity · Diffusivity · Free atmosphere · Inter-component kinetic energy exchange · Kinetic potential and total turbulent energies Monin–Obukhov similarity theory · Stability parameters · Stable stratification · Turbulence closure · Turbulent fluxes · Turbulent dissipation time and length scales

Symbols

$A_i = E_i/E_K$	Share of the i th-component, E_i , of turbulent kinetic energy, E_K
$E = E_K + E_P$	Total turbulent energy (TTE)
$E_K = \frac{1}{2} \langle u_i u_i \rangle$	Turbulent kinetic energy (TKE)
E_i	Longitudinal ($i = 1$ or $i = x$), transverse ($i = 2$ or $i = y$) and vertical ($i = 3$ or $i = z$) components of TKE
$E_\theta = \frac{1}{2} \langle \theta^2 \rangle$	“Energy” of potential temperature fluctuations
E_P	Turbulent potential energy (TPE), Eq. 28
$F_i = \langle u_i \theta \rangle$	Turbulent flux of potential temperature
F_z	Vertical component of F_i
$f = 2\Omega \sin \varphi$	Coriolis parameter
\mathbf{g}	Acceleration due to gravity
K_M	Eddy viscosity, Eq. 43
K_H	Eddy conductivity, Eq. 44
K_D	Eddy diffusivity
L	Obukhov length scale, Eq. 41
l	Turbulent length scale
N	Mean-flow Brunt–Väisälä frequency
P	Mean pressure
P_0	Reference value of P
p	Fluctuation of pressure
$Pr = \nu/\kappa$	Prandtl number
Pr_T	Turbulent Prandtl number, Eq. 45
Q_{ij}	Correlations between fluctuations of pressure and velocity shear, Eq. 15
Ri	Gradient Richardson number, Eq. 3
Ri_f	Flux Richardson number, Eq. 40
R_∞	Maximal Ri in homogeneous sheared flow
$S = \partial \mathbf{U} / \partial z $	Vertical shear of the horizontal mean wind
T	Absolute temperature
T_0	Reference value of absolute temperature
$t_T = lE_K^{-1/2}$	Dissipation time scale
t_τ	Effective dissipation time scale
$\mathbf{U} = (U_1, U_2, U_3)$	Mean wind velocity
$\mathbf{u} = (u_1, u_2, u_3)$	Velocity fluctuation
$\beta = g/T_0$	Buoyancy parameter
$\gamma = c_p/c_v$	Ratio of specific heats at constant pressure and constant volume

$\varepsilon_K, \varepsilon_\theta, \varepsilon_i^{(F)}$ and $\varepsilon_{ij}^{(\tau)}$	Dissipation rates for $E_K, E_\theta, F_i^{(F)}$ and τ_{ij}
$\varepsilon_{\alpha 3}^{(\tau)}$ ($\alpha = 1, 2$)	Effective dissipation rates for the vertical turbulent fluxes of momentum
κ	Temperature conductivity
ν	Kinematic viscosity
$\Pi = E_P/E_K$	Energy stratification parameter, Eq. 74
Φ_K, Φ_θ and Φ_F	Third-order turbulent fluxes of TKE E_K , and the fluxes of E_θ and F_i
φ	Latitude
τ_{ij}	Reynolds stresses (components of turbulent flux of momentum)
$\tau_{\alpha 3}$ ($\alpha = 1, 2$)	Components of the Reynolds stresses representing the vertical turbulent flux of momentum
τ	Modulus of the horizontal vector (τ_{13}, τ_{23})
ρ	Mean density
ρ_0	Reference value of ρ
Θ	Mean potential temperature
θ	Fluctuation of potential temperature
Ω	Angular velocity of Earth's rotation
Ω_i	Earth's rotation vector (parallel to the polar axis)

Basic empirical dimensionless constants of the EFB closure

$C_0 = 0.125$	Inter-component energy exchange constant determining the vertical share of TKE, Eqs. 49, 50c
$C_1 = 0.5, C_2 = 0.72$	Inter-component energy exchange constants determining the longitudinal and transverse shares of TKE, Eqs. 48–50
$C_F = 0.25$	Dissipation time scale constant for the turbulent flux of potential temperature, Eq. 19
$C_P = 0.86$	Dissipation time-scale constant for the turbulent flux of TPE, Eq. 19
$C_r = 1.5$	Standard inter-component energy exchange constant, Eqs. 27, 50a, 50b, 50c
$C_\tau = 0.2$	Dissipation time-scale constant for the turbulent flux of momentum, Eq. 33
$C_\Omega = 1$	Rotational length-scale constant, Eq. 73
$R_\infty = 0.25$	Upper limit for the flux Richardson number attainable in the steady-state regime of turbulence, Eqs. 40, 46
$k = 0.4$	von Karman constant, Eq. 67

Additional constants expressed through the basic constants

$a_1 = 0.18, a_2 = 0.16, a_3 = 1.42$	in Eqs. 81–86
$C_u = k/R_\infty = 1.6$	In the velocity gradient formulation, Eq. 70
$C_\theta = 0.105$	In Eqs. 36, 37, 47, 64
$k_T = (C_F/C_\tau)k = 0.5$	von Karman constant for temperature, Eq. 86
$Pr_T^{(0)} = 0.8$	Turbulent Prandtl number in neutral stratification, Eq. 57
$\Pi_\infty = 0.14$	Upper limit for the energy stratification parameter, Eq. 76

1 Introduction

Historical overviews of the turbulence closure problem and recent developments in this area of knowledge have been discussed during the last decade by [Canuto \(2002, 2009\)](#), [Canuto et al. \(2001, 2005, 2008\)](#), [Cheng et al. \(2002\)](#), [Kurbatsky and Kurbatskaya \(2006, 2009, 2010\)](#) and [Zilitinkevich et al. \(2007, 2008, 2009\)](#). Most of the operationally used closures employ the concept of the downgradient turbulent transport, implying that the vertical turbulent fluxes of momentum τ_i ($i = 1, 2$), potential temperature F_z and other scalars are proportional to their mean gradients. The proportionality coefficients in such relations, called the eddy viscosity K_M , eddy conductivity K_H and eddy diffusivity K_D , are just the unknowns to be determined from the turbulence closure theory. The modern content of this theory originates from [Kolmogorov \(1941, 1942\)](#). He employed the budget equation for the turbulent kinetic energy per unit mass (TKE) E_K to quantify the intensity of turbulence, and postulated that the turbulent exchange coefficients K_M , K_H and K_D are fully characterized by the turbulent velocity scale u_T , where $u_T = E_K^{1/2}$, and the turbulent time scale t_T , defined as the ratio $t_T = E_K/\varepsilon_K$ (where ε_K is the TKE dissipation rate). This concept yields the relations:

$$\varepsilon_K = \frac{E_K}{t_T}, \quad (1)$$

$$K_M \sim K_H \sim K_D \sim u_T^2 t_T \sim u_T l, \quad (2)$$

where $l = E_K^{1/2} t_T$ is the turbulent length scale, whereas the omitted proportionality coefficients in Eq. 2 are assumed to be universal dimensionless constants.

This approach, although quite successful when applied to neutrally stratified flows, is not quite applicable to stable stratification. Indeed, Eq. 2 implies that the turbulent Prandtl number $Pr_T \equiv K_M/K_H$ is nothing but a universal constant. In the context of the Kolmogorov type closures based on the sole use of the TKE budget equation, this inevitably implies the total decay of turbulence already at moderately stable stratification. However, numerous experiments, large-eddy simulations (LES) and direct numerical simulations (DNS) demonstrate that Pr_T drastically increases with increasing static stability (see Fig. 5 below) and, moreover, that turbulence is continuously maintained by the velocity shear even in very stable stratification. This contradiction was overtaken heuristically, prescribing essentially different stability dependences of the turbulent length scales for momentum l_M and heat l_H (and, therefore, for the time scales t_M and t_H). In so doing, the Kolmogorov turbulence closure, originally formulated and justified for neutrally stratified boundary-layer flows (where l can be taken proportional to the distance, z , over the surface) factually became unclosed.

In the energy- and flux-budget (EFB) closure ([Zilitinkevich et al. 2007, 2008, 2009](#)) we refined budget equations for the basic second moments: the two energies, the TKE E_K and the turbulent potential energy (TPE) E_P , and the vertical turbulent fluxes of momentum and potential temperature, τ_i ($i = 1, 2$) and F_z ; removed the artificial turbulence cut-off in the “supercritical” stratification (inherent to the “one energy equation approach”); and, instead of the traditional postulation of the down-gradient turbulent transport, derived the flux-profile relationships and determined the eddy viscosity and eddy conductivity from the steady-state version of the budget equations for τ_i and F_z .

In the present paper we further advance the physical background of the EFB closure, introduce a new prognostic equation for the turbulent dissipation time scale t_T , and extend the theory to non-steady turbulence regimes accounting for non-gradient and non-local turbulent transports (when the traditional concepts of eddy viscosity and eddy conductivity become generally inconsistent).

In Sect. 2, we refine our approximation of the basic energy- and flux-budget equations, in particular, accounting for the difference between the dissipation time scales for TKE and TPE. In Sect. 3, focused on the steady-state (algebraic) version of the closure, we develop a new model of the inter-component exchange of TKE (instead of the traditional hypothesis of “return-to-isotropy” shown to be inconsistent with modern experimental evidence); clarify the concept of the turbulent dissipation time scale and determine its stability dependence; demonstrate how the steady-state version of the EFB closure relates to the Monin and Obukhov (1954) similarity theory; verify the EFB closure against available empirical data, and determine dimensionless universal constants of the theory. In Sect. 4, we extend the theory to non-steady regimes of turbulence; introduce a relaxation equation for the turbulent dissipation time scale; and propose a hierarchy of the EFB closure models including its most general version based on prognostic equations for all essential parameters of turbulence: E_K , E_P , τ_i , F_z and t_T , and simpler versions employing the concepts of eddy viscosity and eddy conductivity.

We recall that the background stratification of density is characterized by the gradient Richardson number:

$$Ri \equiv \frac{N^2}{S^2}, \quad (3)$$

where S and N are the velocity shear and the Brunt–Väisälä frequency:

$$S^2 = \left(\frac{\partial U}{\partial z} \right)^2 + \left(\frac{\partial V}{\partial z} \right)^2, \quad (4)$$

$$N^2 = \frac{g}{\rho_0} \frac{\partial \rho}{\partial z} = \beta \frac{\partial \Theta}{\partial z}. \quad (5)$$

Here, z is the height; U and V are the mean velocity components along the horizontal axes x and y , ρ is the mean density, ρ_0 is its reference value, $g = 9.81 \text{ m s}^{-1}$ is the acceleration due to gravity, $\beta = g/T_0$ is the buoyancy parameter, Θ is the mean potential temperature linked to the absolute temperature T by the relation: $\Theta = T(P_0/P)^{1-1/\gamma}$, where P is the pressure, P_0 and T_0 are reference values of P and T , and $\gamma = c_p/c_v = 1.41$ is the ratio of specific heats. In dry air $\rho = \beta\Theta$, so that the density stratification is fully controlled by the vertical gradient of potential temperature.

Since Richardson (1920), it was generally believed that in stationary homogeneous flows the velocity shear becomes incapable of maintaining turbulence (which therefore collapses) when Ri exceeds some critical value, Ri_c (with the conventional value of $Ri_c = 0.25$). On the contrary, in atmospheric and oceanic modelling, the turbulence cut-off at “supercritical” values of Ri was understood as an obvious artefact and prevented with the aid of “correction coefficients” specifying the ratios $K_M/(u_T l)$ and $K_H/(u_T l)$ as essentially different functions of Ri (Mellor and Yamada 1974). The EFB closure automatically accounts for the maintenance of turbulence by the velocity shear at any Ri and does not require any artificial tricks to prevent the turbulence cut-off. It does not imply any critical Ri in the traditional sense (as the boundary between turbulent and laminar regimes) but discloses, just around $Ri \approx 0.2$ – 0.3 , quite a sharp transition between the two turbulent regimes of principally different natures: strong turbulence at small Ri and weak turbulence at large Ri . Following the EFB closure (Elperin et al. 2005; Zilitinkevich et al. 2007), other recently published turbulent closure models (Mauritsen et al. 2007; Canuto et al. 2008; L’vov et al. 2008; Sukoriansky and Galperin 2008) also do not imply a critical Richardson number.

2 Basic Equations

2.1 Geophysical Approximation

Below we formulate the EFB closure in terms of atmospheric flows characterized by the following typical features:

- Vertical scales of motions (maximum ≈ 10 km) are much smaller than horizontal scales ($\sim 10^3$ – 10^4 km), which is why the mean-flow vertical velocity, W , is orders of magnitude smaller than the horizontal velocities, U and V . Hence the vertical turbulent transports are comparable with or even dominate the mean flow vertical advection, whereas the streamwise horizontal turbulent transport is usually negligible compared to the horizontal advection.
- Typical vertical gradients (along the x_3 or z axis) of the mean wind velocity $\mathbf{U}=(U_1, U_2, U_3)=(U, V, W)$, potential temperature Θ and other variables are orders of magnitude larger than the horizontal gradients (along the x_1, x_2 or x, y axes). Hence, direct effects of the mean-flow horizontal gradients on turbulent statistics are negligible, and the TKE generation is controlled almost entirely by the two components of the velocity gradient: $\partial U/\partial z$ and $\partial V/\partial z$.

Therefore only the components $\tau_{13} = \langle uw \rangle$, $\tau_{23} = \langle vw \rangle$ of the Reynolds stresses $\tau_{ij} = \langle u_i u_j \rangle$ and the vertical component $F_3 = F_z = \langle \theta w \rangle$ of the potential temperature flux $F_i = \langle \theta u_i \rangle$ are needed to close the Reynolds-averaged momentum equations:

$$\frac{DU}{Dt} = fV - \frac{1}{\rho_0} \frac{\partial P}{\partial x} - \frac{\partial \tau_{13}}{\partial z}, \tag{6}$$

$$\frac{DV}{Dt} = -fU - \frac{1}{\rho_0} \frac{\partial P}{\partial y} - \frac{\partial \tau_{23}}{\partial z}, \tag{7}$$

and the thermodynamic energy equation:

$$\frac{D\Theta}{Dt} = -\frac{\partial F_z}{\partial z} + J. \tag{8}$$

Here, $D/Dt = \partial/\partial t + U_k \partial/\partial x_k$, t is time, $f = 2\Omega \sin \varphi$ is the Coriolis parameter, Ω_i is the Earth’s rotation vector parallel to the polar axis ($|\Omega_i| \equiv \Omega = 0.76 \times 10^{-4} \text{ s}^{-1}$), φ is the latitude, ρ_0 is the mean density, J is the heating/cooling rate ($J = 0$ in adiabatic processes), P is the mean pressure, $\mathbf{u}=(u_1, u_2, u_3) = (u, v, w)$ and θ are the velocity and the potential-temperature fluctuations; and angle brackets denote the ensemble-averaged values [see e.g. Holton 2004; Kraus and Businger 1994]. Generally, atmospheric dynamics problems include the specific-humidity equation (analogous to Eq. 8), which involves the vertical turbulent flux of humidity F_q contributing to the vertical turbulent flux of buoyancy: $F_z \beta + 0.61g F_q$. As concerns the turbulence closure, this does not cause additional problems.

General forms of the budget equations for the Reynolds stress, potential-temperature flux and the “energy” of the potential temperature fluctuations $E_\theta = \langle \theta^2 \rangle / 2$ are

$$\frac{D\tau_{ij}}{Dt} + \frac{\partial}{\partial x_k} \Phi_{ijk}^{(\tau)} = -\tau_{ik} \frac{\partial U_j}{\partial x_k} - \tau_{jk} \frac{\partial U_i}{\partial x_k} - \left[\varepsilon_{ij}^{(\tau)} - \beta(F_j \delta_{i3} + F_i \delta_{j3}) - Q_{ij} \right], \tag{9}$$

$$\frac{DF_i}{Dt} + \frac{\partial}{\partial x_j} \Phi_{ij}^{(F)} = \beta \delta_{i3} \langle \theta^2 \rangle - \frac{1}{\rho_0} \langle \theta \nabla_i p \rangle - \tau_{ij} \frac{\partial \Theta}{\partial z} \delta_{j3} - F_j \frac{\partial U_i}{\partial x_j} - \varepsilon_i^{(F)}, \tag{10}$$

$$\frac{DE_\theta}{Dt} + \nabla \cdot \Phi_\theta = -F_z \frac{\partial \Theta}{\partial z} - \varepsilon_\theta, \tag{11}$$

where δ_{ij} is the unit tensor ($\delta_{ij} = 1$ for $i = j$ and $\delta_{ij} = 0$ for $i \neq j$); see, e.g., [Kaimal and Finnigan \(1994\)](#), [Kurbatsky \(2000\)](#) and [Cheng et al. \(2002\)](#). Other notations in Eqs. 9–11 are as follows:

$\Phi_{ijk}^{(\tau)}$, Φ_{ij}^F and Φ_θ are the third-order moments describing turbulent transports of the second-order moments:

$$\Phi_{ijk}^{(\tau)} = \langle u_i u_j u_k \rangle + \frac{1}{\rho_0} (\langle p u_i \rangle \delta_{jk} + \langle p u_j \rangle \delta_{ik}), \tag{12}$$

$$\Phi_{ij}^{(F)} = \langle u_i u_j \theta \rangle + \frac{1}{2\rho_0} \langle p \theta \rangle \delta_{ij}, \tag{13}$$

$$\Phi_\theta = \frac{1}{2} \langle \theta^2 \mathbf{u} \rangle, \tag{14}$$

Q_{ij} are correlations between fluctuations of the pressure, p , and the velocity shear, $\partial u_i / \partial x_j$:

$$Q_{ij} = \frac{1}{\rho_0} \left\langle p \left(\frac{\partial u_i}{\partial x_j} + \frac{\partial u_j}{\partial x_i} \right) \right\rangle, \tag{15}$$

$\varepsilon_{ij}^{(\tau)}$, $\varepsilon_i^{(F)}$ and ε_θ are the terms associated with the kinematic viscosity ν and the temperature conductivity κ :

$$\varepsilon_{ij}^{(\tau)} = 2\nu \left\langle \frac{\partial u_i}{\partial x_k} \frac{\partial u_j}{\partial x_k} \right\rangle, \tag{16}$$

$$\varepsilon_i^{(F)} = -\kappa (\langle u_i \Delta \theta \rangle + Pr \langle \theta \Delta u_i \rangle), \tag{17}$$

$$\varepsilon_\theta = -\kappa \langle \theta \Delta \theta \rangle, \tag{18}$$

where $Pr = \nu/\kappa$ is the Prandtl number.

The terms $\varepsilon_{ii}^{(\tau)}$, $\varepsilon_i^{(F)}$ and ε_θ are essentially positive and represent the dissipation rates of the statistical moments under consideration. Following [Kolmogorov \(1941, 1942\)](#) they are determined as the ratios of the moments to their dissipation time scale, t_Γ :

$$\varepsilon_{ii}^{(\tau)} = \frac{\tau_{ii}}{t_\Gamma}, \quad \varepsilon_i^{(F)} = \frac{F_i}{C_F t_\Gamma}, \quad \varepsilon_\theta = \frac{E_\theta}{C_P t_\Gamma}, \tag{19}$$

where $\tau_{ii} \equiv \langle u_i^2 \rangle$, C_P and C_F are dimensionless universal constants quantifying the difference between the dissipation time scales for different moments. All these time scales are taken proportional to the master time scale t_Γ .

2.2 EFB Model Equations

From this point onwards we limit our analysis to the geophysical approximation and basically follow [Zilitinkevich et al. \(2007, 2008, 2009\)](#). The diagonal terms of the Reynolds stress tensor $\tau_{ii} \equiv \langle u_i^2 \rangle$ make doubled components of TKE: $E_i \equiv \langle u_i^2 \rangle / 2$, and their budgets are expressed by Eq. 9 for $i = j$:

$$\frac{DE_i}{Dt} + \frac{\partial}{\partial z} \Phi_i = -\tau_{i3} \frac{\partial U_i}{\partial z} + \frac{1}{2} Q_{ii} - \frac{E_i}{t_\Gamma} \quad (i = 1, 2), \tag{20}$$

$$\frac{DE_z}{Dt} + \frac{\partial}{\partial z} \Phi_z = \beta F_z + \frac{1}{2} Q_{33} - \frac{E_z}{t_\Gamma}, \tag{21}$$

where

$$\Phi_i = \frac{1}{2} \langle u_i^2 w \rangle \quad (i = 1, 2), \tag{22}$$

$$\Phi_3 = \frac{1}{2} \langle w^3 \rangle + \frac{1}{\rho_0} \langle p w \rangle. \tag{23}$$

Summing up Eqs. 20 and 21, yields the familiar TKE budget equation:

$$\frac{DE_K}{Dt} + \frac{\partial}{\partial z} \Phi_K = -\tau_{i3} \frac{\partial U_i}{\partial z} + \beta F_z - \frac{E_K}{t_T}, \tag{24}$$

where the third term on the right-hand side (r.h.s.) represents the TKE dissipation rate:

$$\varepsilon_K = \frac{E_K}{t_T}, \tag{25}$$

and Φ_K represents the vertical turbulent flux of TKE:

$$\Phi_K = \frac{1}{2} \langle u_i u_i w \rangle + \frac{1}{\rho_0} \langle p w \rangle. \tag{26}$$

The sum of the terms Q_{ii} (the trace of the tensor Q_{ij}) vanishes because of the continuity equation: $\partial u_i / \partial x_i = 0$. Hence, these terms are neither productive nor dissipative and describe the kinetic energy exchange between the “richer” component (fed by shear) and the “poorer” transverse and vertical components. Traditionally they were determined through the “return-to-isotropy” hypothesis (Rotta 1951):

$$Q_{ii} = -\frac{2C_r}{3t_T} (3E_i - E_K), \tag{27}$$

where the coefficient C_r was treated as a universal dimensionless constant accounting for the difference between the energy-transfer and the energy-dissipation time scales. As revealed in our prior papers, this formulation serves as a reasonable approximation only in neutral and near-neutral stratification but becomes unrealistic in pronounced stable stratification. In particular, it implies that the share of the transverse velocity fluctuations E_y/E_K does not depend on Ri , whereas in reality it significantly increases with increasing Ri so that E_y/E_K and E_x/E_K gradually approach each other (see Fig. 3 below). In the present paper we develop a new energy exchange concept accounting for this effect and retain Eq. 27 only for neutral stratification.

Although the budget equation for the squared fluctuation of potential temperature E_θ , Eq. 11, was known over decades (see Lumley and Panofsky 1964; Tennekes and Lumley 1972), its crucial importance for the turbulence energetics was long overlooked. Ostrovsky and Troitskaya (1987) and more recently Zilitinkevich et al. (2007) emphasized the close relation between E_θ and the TPE. For the background of stable stratification characterized by the Brunt–Väisälä frequency N , the vertical displacement of a fluid parcel from its initial level z to the level $z + \delta z$ causes the density increment $\delta \rho = (\partial \rho / \partial z) \delta z = (\rho_0 / g) N^2 \delta z$, where ρ is the mean density. Then the increment in potential energy per unit mass $\delta E_P = (1 / \delta z) \int_z^{z+\delta z} (g / \rho_0) \delta \rho z dz$ is expressed as $\delta E_P = \frac{1}{2} [(g / \rho_0) \delta \rho]^2 / N^2 = \frac{1}{2} (\beta \delta \theta)^2 / N^2 = (\beta / N)^2 \delta E_\theta$, where $\delta E_\theta = \frac{1}{2} (\delta \theta)^2$ is the increment in the “energy” of the potential temperature fluctuations. This yields the expression for the TPE:

$$E_P = \left(\frac{\beta}{N} \right)^2 E_\theta. \tag{28}$$

In contrast to the potential energy of the mean flow, which depends on the temperature variation linearly, the TPE is proportional to the squared temperature fluctuation. This reminds us of the concept of available potential energy determined by Lorenz (1955) as that part of the total potential energy of the general circulation available for conversion into kinetic energy. The same is true for the TPE: it is just the potential energy that can be converted into TKE and vice versa.

In a geophysical approximation, the budget equation for E_θ , Eq. 11, and the corresponding equation for E_P read:

$$\frac{DE_\theta}{Dt} + \frac{\partial}{\partial z} \Phi_\theta = -F_z \frac{\partial \Theta}{\partial z} - \frac{E_\theta}{C_p t_T}, \tag{29}$$

$$\frac{DE_P}{Dt} + \frac{\partial}{\partial z} \Phi_P = -\beta F_z - \frac{E_P}{C_p t_T}, \tag{30}$$

where Φ_θ and Φ_P are the third-order turbulent fluxes of the second-order fluxes E_θ and E_P , respectively:

$$\Phi_P = \left(\frac{\beta}{N}\right)^2 \Phi_\theta = \frac{1}{2} \left(\frac{\beta}{N}\right)^2 \langle \theta^2 w \rangle. \tag{31}$$

The last terms on the r.h.s. of Eqs. 29 and 30 are the dissipation rates: $\varepsilon_\theta = E_\theta / (C_p t_T)$ and $\varepsilon_P = E_P / (C_p t_T)$.

The buoyancy flux, βF_z , appears in Eqs. 24 and 30 with opposite signs and describes nothing but the energy exchange between TKE and TPE. In the budget equation for the total turbulent energy (TTE = TKE + TPE), defined as

$$E = E_K + E_P = \frac{1}{2} \left(\langle u_i u_i \rangle + \left(\frac{\beta}{N}\right)^2 \langle \theta^2 \rangle \right), \tag{32}$$

the terms $\pm \beta F_z$ cancel each other. Thus there are no grounds to consider the buoyancy-flux term in the TKE equation as an ultimate “killer” of turbulence.

In Eq. 9 for the vertical components of the turbulent flux of momentum, τ_{i3} ($i = 1, 2$), the molecular-viscosity term, $\varepsilon_{i3}^{(\tau)}$, is small (because the smallest eddies associated with viscous dissipation are presumably isotropic; see Lvov et al. 2009), and the dissipative role is played by the combination of terms $\varepsilon_{i3}^{(\tau)(\text{eff})} = -\beta F_i - Q_{i3}$. Zilitinkevich et al. (2007) called this combination the “effective dissipation rate” and expressed it through the Kolmogorov closure hypothesis:

$$\varepsilon_{i3}^{(\tau)(\text{eff})} \equiv -\beta F_i - Q_{i3} = \frac{\tau_{i3}}{C_\tau t_T} = \frac{\tau_{i3} \varepsilon_K}{C_\tau E_K}, \tag{33}$$

where C_τ is the effective-dissipation time-scale constant. Then the budget equation for τ_{i3} ($i = 1, 2$) simplifies to

$$\frac{D\tau_{i3}}{Dt} + \frac{\partial}{\partial z} \Phi_i^{(\tau)} = -2E_z \frac{\partial U_i}{\partial z} - \frac{\tau_{i3}}{C_\tau t_T}, \tag{34}$$

where $\Phi_i^{(\tau)}$ is the vertical turbulent flux of τ_{i3} :

$$\Phi_i^{(\tau)} = \langle u_i w^2 \rangle + \frac{1}{\rho_0} \langle p u_i \rangle. \tag{35}$$

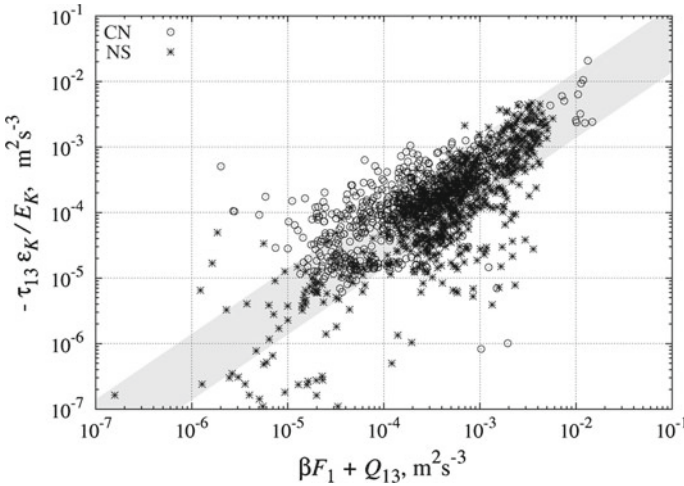


Fig. 1 Comparison of the effective dissipation rate of the momentum flux calculated by its definition (abscissa) and by the Kolmogorov closure hypothesis (ordinate), after LES [our DATABASE64; see [Esau \(2004, 2009\)](#), [Esau and Zilitinkevich \(2006\)](#)] for conventionally neutral (CN) and nocturnal stable (NS) atmospheric boundary layers. The linear dependence (*grey corridor*) corresponds to our approximation, Eq. 33

In [Zilitinkevich et al. \(2007\)](#), the concept of the effective dissipation, Eq. 33, was based on our prior analysis of the Reynolds stress equation in k -space using the familiar “ τ -approximation” ([Elperin et al. 2002, 2006](#)). In Fig. 1 we compare Eq. 33 with data from large-eddy simulation (LES) of the two types of atmospheric boundary layer: “nocturnal stable” (NS, with essentially a negative buoyancy flux at the surface and neutral stratification in the free flow) and “conventionally neutral” (CN, with a negligible buoyancy flux at the surface and essentially stable static stability in the free flow). Admittedly, LES is unable to directly reproduce ε_K , which is why we estimated the r.h.s. of Eq. 33 approximately, taking $\varepsilon_K = -\tau_{13} \partial U_i / \partial z + \beta F_z$ —as it follows from the steady-state version of Eq. 24. In spite of the quite large spread of data points, Fig. 1 confirms that the effective dissipation $\varepsilon_{13}^{(\tau)}$ (ordinate) is basically proportional to the combination $\tau_{13} \varepsilon_K / E_K$ (abscissa). The grey corridor covering most of the data points corresponds to Eq. 33 with $0.1 < C_\tau < 1$, which is consistent with our independent estimate of $C_\tau = 0.2$.

As demonstrated through a scaling analysis in Appendix A of [Zilitinkevich et al. \(2007\)](#), the term $\rho_0^{-1} \langle \theta \partial p / \partial z \rangle$ in Eq. 10 for the vertical turbulent flux of potential temperature F_z can be taken proportional to the mean squared temperature, so that

$$\frac{\rho_0^{-1} \langle \theta \partial p / \partial z \rangle}{\beta \langle \theta^2 \rangle} = 1 - C_\theta, \tag{36}$$

where $C_\theta = \text{constant} < 1$. In Fig. 2 we compare this hypothetical relation with data from LES. Most of the data points (grey corridor) confirm Eq. 36. Then Eq. 10 simplifies to

$$\frac{DF_z}{Dt} + \frac{\partial}{\partial z} \Phi_z^{(F)} = -2(E_z - C_\theta E_P) \frac{\partial \Theta}{\partial z} - \frac{F_z}{C_{FT}}. \tag{37}$$

Equations 20, 21, 24 determine the turbulent kinetic energies E_i ($i = 1, 2, 3$) and E_K ; Eqs. 29, 30 determine the “energy” of the temperature fluctuations E_θ and the TPE E_P ; Eqs. 34, 37 determine the vertical turbulent fluxes of momentum τ_{i3} ($i = 1, 2$) and potential

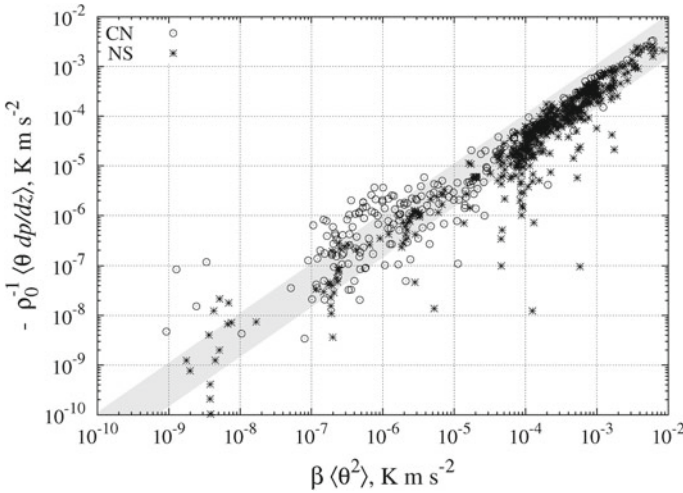


Fig. 2 Comparison of the first (abscissa) and the second (ordinate) terms on the r.h.s. of Eq. 10, after LES (our DATABASE64). The linear dependence (*grey corridor*) corresponds to our approximation, Eq. 36

temperature F_z . More specifically, the vertical TKE E_z is determined in Sect. 3.2. The turbulent dissipation time scale τ_T is determined in Sect. 3.4, and the prognostic equation for τ_T closing the above system is proposed in Sect. 4.1.

3 Steady-State Regime of Turbulence

3.1 Stability Parameters, Eddy Viscosity and Eddy Conductivity

We consider the EFB model in its simplest, algebraic form, neglecting non-steady terms in all budget equations. In the TKE budget Eq. 24 the first term on the r.h.s. is the rate of the TKE production:

$$-\tau_{i3} \frac{\partial U_i}{\partial z} = \tau S, \tag{38}$$

where τ and S are absolute values of the vectors $\boldsymbol{\tau} = (\tau_{xz}, \tau_{yz})$ and $\mathbf{S} = (\partial U/\partial z, \partial V/\partial z)$; and the second term βF_z is the rate of conversion of TKE into TPE. The ratio of these terms, termed the “flux Richardson number”:

$$Ri_f \equiv \frac{-\beta F_z}{\tau S}, \tag{39}$$

characterizes the effect of stratification on turbulence similar to the gradient Richardson number Ri , Eq. 3. Clearly, Ri_f can also be treated as the ratio of the velocity-shear length scale $\tau^{1/2}/S$ to the Obukhov (1946) stratification length scale L :

$$Ri_f = \frac{\tau^{1/2}}{SL}, \tag{40}$$

where L is defined as

$$L = \frac{\tau^{3/2}}{-\beta F_z}. \tag{41}$$

Furthermore, the dimensionless height

$$\zeta = z/L \tag{42}$$

characterizes the effect of stratification similar to Ri or Ri_f (Monin and Obukhov 1954).

The steady-state versions of the budget equations, Eqs. 34 and 37, for the vertical turbulent fluxes τ_{i3} and F_z for the momentum and the potential temperature, yield the flux-gradient relations that can be expressed in terms of the eddy viscosity K_M and eddy conductivity K_H :

$$\tau_{i3} = -K_M \frac{\partial U_i}{\partial z}, \quad K_M = 2C_\tau E_z t_T, \tag{43}$$

$$F_z = -K_H \frac{\partial \Theta}{\partial z}, \quad K_H = 2C_F t_T E_z \left(1 - C_\theta \frac{E_P}{E_z} \right). \tag{44}$$

The latter relations yield the following expression for the turbulent Prandtl number:

$$Pr_T \equiv \frac{K_M}{K_H} \equiv \frac{Ri}{Ri_f} = \frac{C_\tau}{C_F} \left(1 - C_\theta \frac{E_P}{E_z} \right)^{-1}. \tag{45}$$

It is clearly seen from the steady-state version of the TKE budget, Eq. 24, that Ri_f in the steady-state regime can only increase with increasing Ri , but obviously cannot exceed unity. Hence it should tend to a finite asymptotic limit (estimated in Sect. 3.3 as $R_\infty = 0.25$), which corresponds to the asymptotically linear Ri dependence of Pr_T :

$$Ri_f \rightarrow R_\infty, \quad Pr_T \rightarrow \frac{Ri}{R_\infty} \text{ at } Ri \rightarrow \infty. \tag{46}$$

Similar reasoning, including the approximation of $Pr_T \approx Pr_T^{(0)} + Ri/R_\infty$ for $Ri \gg 1$, and the estimate of $R_\infty \approx 0.25$, have already been proposed by Schumann and Gerz (1995). Because $Pr_T \rightarrow \infty$ at $Ri \rightarrow \infty$, it follows from Eq. 45 that the constant C_θ (Eqs. 36–37) satisfies the relation

$$C_\theta = (E_z/E_P)_{Ri \rightarrow \infty}, \tag{47}$$

and therefore is expressed through to other EFB-model constants.

As is evident from the above analysis, the concepts of eddy viscosity and eddy conductivity are justified only in the steady state, when the left-hand sides (l.h.s.) of the flux budget equations, Eqs. 34 and 37, can be neglected.

3.2 Inter-Component Exchange of Turbulent Kinetic Energy

In the geophysical flows under consideration, the mean wind shear generates the energy of the longitudinal velocity fluctuations E_x , which feeds the transverse E_y and the vertical E_z energy components. The inter-component energy exchange term in the momentum-flux budget equation, Eq. 9, namely Q_{ij} specified by Eq. 15, is traditionally parametrized through the Rotta (1951) “return-to-isotropy” hypothesis, Eq. 27. In combination with the energy budget Eqs. 20 and 21, it results in expressions of the longitudinal, $A_x = E_x/E_K$, transverse, $A_y = E_y/E_K$, and vertical, $A_z = E_z/E_K$, shares of TKE characterized by the following features: (i) in neutral stratification $A_z = A_y$; (ii) with strengthening stability A_x increases at the expense of A_z (which therefore decreases), while A_y does not depend on stratification.

However, these features are inconsistent with modern experimental evidence. Available atmospheric data demonstrate that, (i) in neutral stratification $A_z^{(0)} \equiv A_z|_{\zeta=0}$ is essentially smaller than $A_y^{(0)} \equiv A_y|_{\zeta=0}$, (ii) with strengthening stability A_y increases and A_x decreases,

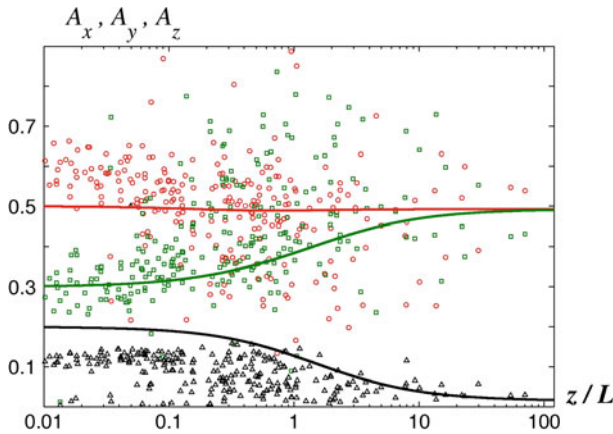


Fig. 3 The shares of the turbulent kinetic energy E_K : longitudinal $A_x = E_x/E_K$ (along the mean wind, red circles), transverse $A_y = E_y/E_K$ (green squares) and vertical $A_z = E_z/E_K$ (black triangles), after the Kalmykia-2007 field campaign of the A.M. Obukhov Institute of Atmospheric Physics of the Russian Academy of Sciences (courtesy of Rostislav Kouznetsov). The lines show our inter-component energy exchange model, Eq. 50, with $C_0 = 0.125$, $C_1 = 0.5$ and $C_2 = 0.72$, converted into z/L dependences with the aid of Eq. 71

tending towards horizontal isotropy: $A_y \rightarrow A_x$, (iii) the vertical energy share, A_z , generally decreases with increasing $\zeta = z/L$, and at $\zeta > 1$ levels off at a quite small but non-zero limit (see for example Fig. 3). It is conceivable that the stable stratification, suppressing the energy of the vertical velocity E_z , facilitates the energy exchange between the horizontal velocity energies E_y and E_x , and thereby causes a tendency towards isotropy in the horizontal plane. This newly revealed feature calls for revision of the traditional concept of “return-to-isotropy”.

We characterize the static stability by the normalized flux Richardson number, Ri_f/R_∞ , varying from zero in neutral stratification to 1 in extremely stable stratification, and propose the following model reflecting the above principal features of the TKE redistribution between the velocity components:

$$Q_{11} = -\frac{2C_r}{t_T} \left(E_x - \frac{1 - C_1 - C_2 Ri_f/R_\infty}{3} E_{\Leftrightarrow} \right), \tag{48a}$$

$$Q_{22} = -\frac{2C_r}{t_T} \left(E_y - \frac{1 + C_1 + C_2 Ri_f/R_\infty}{3} E_{\Leftrightarrow} \right), \tag{48b}$$

$$Q_{33} = -\frac{2C_r}{t_T} \left(E_z - E_K + \frac{2}{3} E_{\Leftrightarrow} \right), \tag{48c}$$

where E_{\Leftrightarrow} is that part of the TKE participating in the inter-component energy exchange:

$$E_{\Leftrightarrow} = \left(1 + C_0 \frac{Ri_f}{R_\infty} \right) E_K - (1 + C_0) \frac{Ri_f}{R_\infty} E_z. \tag{49}$$

Substituting the energy exchange model, Eqs. 48–49, in the steady-state version of the energy-budget equations 20, 21 yields:

$$A_x = \frac{1}{(1+C_r)(1-Ri_f)} + \left(1 - C_1 - C_2 \frac{Ri_f}{R_\infty}\right) \frac{C_r}{3(1+C_r)} \left[1 + \frac{Ri_f}{R_\infty} [C_0 - (1+C_0)A_z]\right], \tag{50a}$$

$$A_y = \left(1 + C_1 + C_2 \frac{Ri_f}{R_\infty}\right) \frac{C_r}{3(1+C_r)} \left[1 + \frac{Ri_f}{R_\infty} [C_0 - (1+C_0)A_z]\right], \tag{50b}$$

$$A_z = \frac{E_z}{E_K} = \frac{C_r(1 - 2C_0 Ri_f/R_\infty)(1 - Ri_f) - 3Ri_f}{(1 - Ri_f)\{3 + C_r[3 - 2(1 + C_0)Ri_f/R_\infty]\}}, \tag{50c}$$

where C_0 , C_1 and C_2 are dimensionless empirical constants. Figure 3 shows the energy shares A_i , determined by Eq. 50 and converted into the z/L dependence using Eq. 71 (Sect. 3.4). Fitting theoretical curves, Eqs. 50a and 50b, to rather scarce data presented in the figure yields tentative estimates of $C_1 = 0.5$ and $C_2 = 0.72$. In our further analyses they are not needed. Of the TKE shares we use only A_z , Eq. 50c, to determine E_z in Eqs. 43 and 44 for the eddy viscosity and eddy conductivity.

According to Eq. 50c, A_z varies between the following limits:

$$A_z |_{Ri=0} = A_z^{(0)} = \frac{C_r}{3(1+C_r)}, \tag{51}$$

$$A_z |_{Ri \rightarrow \infty} = A_z^{(\infty)} = \frac{C_r(1 - 2C_0) - \frac{3R_\infty}{1-R_\infty}}{3 + C_r(1 - 2C_0)}, \tag{52}$$

where the empirical constants C_0 , C_r and R_∞ are determined below.

3.3 Stability Dependencies of the Basic Parameters of Turbulence, and Determination of Empirical Constants

In the steady state, Eqs. 20, 21, 24, 29, 30, 32, 34 and 37 reduce to algebraic system of equations governing local balances between the generation and dissipation terms. Although this system is not closed (until the turbulent time scale t_T is determined), it allows us to determine basic dimensionless parameters of turbulence as universal functions of the gradient Richardson number Ri , Eq. 3.

Combining Eqs. 24, 30 and Eq. 32 yields the following expressions of the shares of TKE and TPE as universal functions of the flux Richardson number:

$$\frac{E_K}{E} = \frac{1 - Ri_f}{1 - (1 - C_p)Ri_f}, \tag{53}$$

$$\frac{E_p}{E} = \frac{C_p Ri_f}{1 - (1 - C_p)Ri_f}. \tag{54}$$

Then using Eq. 47 to determine C_θ :

$$C_\theta = \frac{(1 - R_\infty)A_z^{(\infty)}}{C_p R_\infty}, \tag{55}$$

and combining Eqs. 45, 53–55 we determine the gradient Richardson number Ri and the turbulent Prandtl number Pr_T :

$$Ri = Pr_T Ri_f = \frac{C_r}{C_F} Ri_f \left(1 - \frac{Ri_f(1 - R_\infty)A_z^{(\infty)}}{R_\infty(1 - Ri_f)A_z(Ri_f)}\right)^{-1}. \tag{56}$$

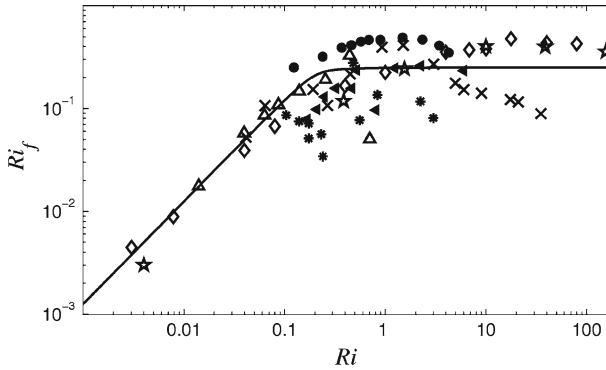


Fig. 4 Ri dependence of the flux Richardson number $Ri_f = -\beta F_z / (\tau S)$ for meteorological observations: slanting black triangles (Kondo et al. 1978), snowflakes (Bertin et al. 1997); laboratory experiments: slanting crosses (Rehmann and Koseff 2004), diamonds (Ohya 2001), black circles (Strang and Fernando 2001); DNS: five-pointed stars (Stretch et al. 2001); LES: triangles (our DATABASE64). Solid line shows the steady-state EFB model, Eq. 56, with $Ri_f \rightarrow R_\infty = 0.25$ at $Ri \rightarrow \infty$

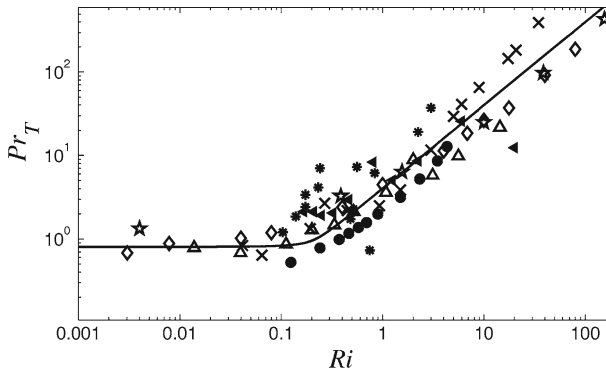


Fig. 5 Ri dependence of the turbulent Prandtl number $Pr_T = K_M / K_H$, after the same data as in Fig. 4 (meteorological observations, laboratory experiments, DNS, and LES). Solid line shows the steady-state EFB model, Eq. 56

Equations 50c, 56 determine Ri as the universal infinitely increasing function of Ri_f and, thereby, implicitly determine

- Ri_f as universal monotonically increasing function of Ri approaching R_∞ at $Ri \rightarrow \infty$;
- and Pr_T as infinitely increasing function of Ri having the asymptote: $Pr_T \rightarrow Ri / R_\infty$ at $Ri \rightarrow \infty$.

Comparison of these functions with data in Figs. 4 and 5 yields quite certain empirical estimate of $R_\infty = 0.25$ (cf. Schumann and Gerz 1995), implying a very strong asymptotic Ri dependence of the turbulent Prandtl number: $Pr_T \approx 4Ri$ at $Ri \gg 1$.

Data for very small Ri in Figs. 4 and 5 are consistent with the well-established empirical value of the turbulent Prandtl number in neutral stratification (e.g., Elperin et al. 1996; Churchill 2002; Foken 2006):

$$Pr_T \rightarrow Pr_T^{(0)} = \frac{C_\tau}{C_F} = 0.8 \quad \text{at } Ri \rightarrow 0. \tag{57}$$

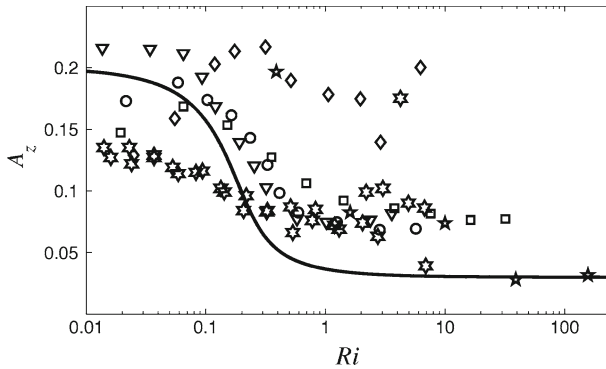


Fig. 6 *Ri* dependence of the vertical share of TKE $A_z = E_z/E_K$, for meteorological observations: squares [CME=Carbon in the Mountains Experiment, Mahrt and Vickers (2005)], circles [SHEBA=Surface Heat Budget of the Arctic Ocean, Uttal et al. (2002)], overturned triangles [CASES-99=Cooperative Atmosphere-Surface Exchange Study, Poulos et al. (2002); Banta et al. (2002)], six-pointed stars [Lindenberg station of the German Weather Service, Engelbart et al. (2000)]; laboratory experiments: diamonds (Ohya 2001); DNS: five-pointed stars (Stretch et al. 2001). Solid line shows the steady-state EFB model, Eqs. 50c and 56, with $C_0 = 0.125$

As follows from Eq. 56 in a linear approximation with respect to *Ri*, the turbulent Prandtl number at $Ri \ll 1$ behaves as

$$Pr_T \approx Pr_T^{(0)} + \frac{(1 - R_\infty)A_z^{(\infty)}}{R_\infty A_z^{(0)}} Ri. \tag{58}$$

Taking empirical values of $R_\infty = 0.25$, $A_z^{(0)} = 0.2$ and $A_z^{(\infty)} = 0.03$ (see Fig. 6 below), Eq. 58 yields $Pr_T \approx 0.8 + 0.45Ri$. This means that Pr_T in the strong-turbulence regime typical of boundary-layer flows varies insignificantly, increasing from 0.8 at $Ri = 0$ –0.9 at $Ri = 0.25$. In the background of the quite natural spread of data, it is practically impossible to recognise such a weak dependence empirically. Over decades, this inherent feature of boundary-layer turbulence has served as a basis for the widely used assumption $Pr_T = \text{constant}$ and given the name “Reynolds analogy”. Our theory justifies it as a reasonable approximation for the strong-turbulence regime ($0 < Ri < 0.25$), and reveals its absolute inapplicability to the weak-turbulence regime ($Ri > 1$), where the *Ri* dependence of Pr_T becomes an order of magnitude stronger: $dPr_T/dRi \approx 4$. Zilitinkevich (2010) has already pointed out the strongly different *Ri* dependences of Pr_T at large and small *Ri* in connection with the conceptual inadequacy of the currently used design of DNS of the stably stratified turbulence for small *Ri*.

Owing to Eq. 56, the above Eqs. 50c, 53 and 54 determine the vertical share of TKE A_z , and the ratios E_K/E and E_P/E as universal functions of *Ri*. Figure 6 shows empirical data on A_z together with theoretical curve plotted after Eq. 50c. Inspection of this figure yields rough estimates of $A_z^{(0)} = 0.2$ and $A_z^{(\infty)} = 0.03$. Consequently, Eq. 51 yields $C_r = 1.5$, and using the above estimate of $R_\infty = 0.25$, Eq. 52 yields $C_0 = 0.125$.

Figure 7 gives an empirical verification of the *Ri* dependence of E_P/E after Eq. 54. At $Ri \rightarrow \infty$ it has the limit:

$$\frac{E_P}{E} \rightarrow \frac{C_P R_\infty}{1 - (1 - C_P)R_\infty}. \tag{59}$$

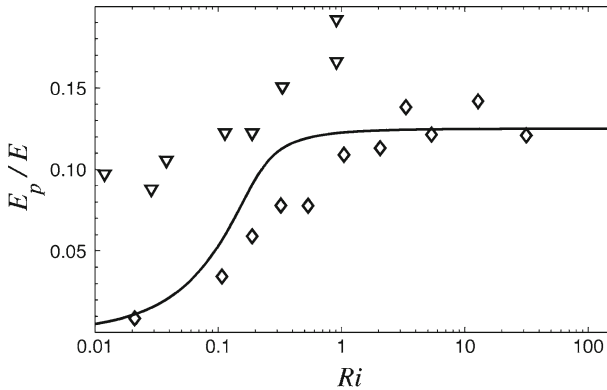


Fig. 7 Ri dependence of the potential-to-total turbulent energy ratio E_p/E , for *meteorological observations: overturned triangles* (CASES-99), and *laboratory experiments: diamonds* (Ohya 2001). Solid line shows the steady-state EFB model, Eqs. 54, 56

Empirical data in Fig. 7 are basically consistent with the curve and allow for estimating the limit: $E_p/E|_{Ri \rightarrow \infty} \rightarrow 0.13$. Using the above estimate of $R_{\infty} = 0.25$, this yields $C_p = 0.86$. We recall that C_p is the ratio of the dissipation time scales for TKE and TPE. Venayagamoorthy and Stretch (2006, 2010) investigated these scales using experimental data on grid-generated turbulence (Srivat and Warhaft 1983; Itsweire et al. 1986; Yoon and Warhaft 1990; Mydlarski 2003) and data from DNS of the stably stratified (Shih et al. 2000) and neutrally stratified (Rogers et al. 1989) homogeneous sheared turbulence. Their analysis demonstrated that the time-scale ratio is relatively insensitive to Ri , which supports our treatment of C_p as a universal constant.

The steady-state version of Eq. 24 together with Eq. 43 yield the following Ri_f dependence of the dimensionless turbulent flux of momentum:

$$\left(\frac{\tau}{E_K}\right)^2 = \frac{2C_\tau A_z(Ri_f)}{(1 - Ri_f)}, \tag{60}$$

while the steady-state version of Eq. 29 together with Eqs. 44–45 yield the Ri_f dependence of the dimensionless turbulent flux of potential temperature:

$$\frac{F_z^2}{E_K E_\theta} = \frac{2C_\tau A_z(Ri_f)}{C_p Pr_T}. \tag{61}$$

Here, the function $A_z(Ri_f)$ is determined from Eq. 50c and the function $Ri_f(Ri)$, from Eq. 56; hence Eq. 60 specifies the Ri dependence of $(\tau/E_K)^2$ and Eq. 61, the Ri dependence of $F_z^2/(E_K E_\theta)$.

Available data on $(\tau/E_K)^2$ together with the theoretical curve plotted after Eq. 60 are shown in Fig. 8. They are consistent with the commonly accepted estimate of $(\tau/E_K)_{Ri \rightarrow 0} = 0.2$ (e.g., Monin and Yaglom 1971) and, in spite of a large spread, confirm a pronounced decrease in τ/E_K with increasing Ri . Using this figure we roughly estimate $2C_\tau A_z^{(0)} = 0.08$ and (using the above empirical value of $A_z^{(0)} = 0.2$) determine $C_\tau = 0.2$.

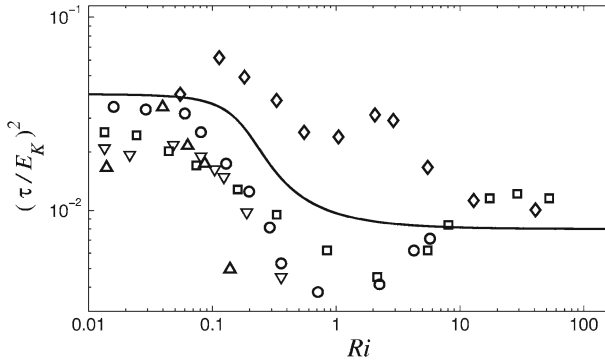


Fig. 8 *Ri* dependence of the squared dimensionless turbulent flux of momentum $(\tau/E_K)^2$, for meteorological observations: squares (CME), circles (SHEBA), overturned triangles (CASES-99); laboratory experiments (Ohya 2001); LES: triangles (our DATABASE64). Solid line shows the steady-state EFB model, Eq. 60

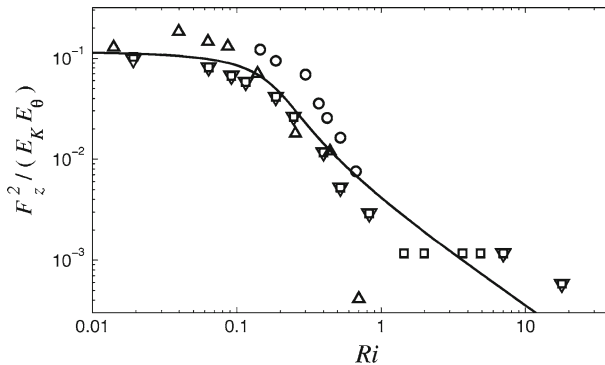


Fig. 9 *Ri* dependence of the squared dimensionless turbulent flux of potential temperature $F_z^2/(E_K E_\theta)$, for meteorological observations: squares (CME), circles (SHEBA), overturned triangles (CASES-99); laboratory experiments: diamonds (Ohya 2001); LES: triangles (our DATABASE64). Solid line shows the steady-state EFB model, Eq. 61

Empirical verification of Eq. 61 shown in Fig. 9 demonstrates a reasonably good correspondence between the theory and data, and allows for determining the small-*Ri* limit:

$$\left(\frac{F_z^2}{E_K E_\theta} \right)_{Ri \rightarrow 0} = \frac{2C_\tau}{C_P} \frac{A_z^{(0)}}{Pr_T^{(0)}} = \frac{2A_z^{(0)} C_F}{C_P} = 0.12, \tag{62}$$

which yields $C_F/C_P = 0.3$. Since $C_P = 0.86$ is already determined, we obtain $C_F = 0.25$.

The above estimates provide empirical values of our basic dimensionless constants:

$$C_0 = 0.125, C_F = 0.25, C_P = 0.86, C_r = 1.5, C_\tau = 0.2, R_\infty = 0.25. \tag{63}$$

We admit that the empirical foundation of these estimates is not quite solid. We deliberately selected datasets shown in different figures to avoid biasing clouds of data points. Our reason is that the algebraic version of the model selected for validation against empirical data is valid only for stationary homogeneous turbulence, whereas available datasets (except DNS of the stably stratified turbulence for given Richardson numbers) basically correspond to heterogeneous and/or non-stationary turbulence. Our estimation of the empirical constants

from quite limited and not fully reliable datasets is to some extent justified by the facts that the constants are interdependent (changing one of them we are forced to change all others), and the number of constants is less than the number of the employed empirical dependencies. This made it possible to determine the entire set of constants searching for the optimal solution to the over-determined set of algebraic relations expressing the unknown constants through the measurable parameters.

As follows from Eq. 47, the constant $C_\theta = \lim(E_z/E_P) |_{Ri \rightarrow \infty}$ is not independent. Then the identity $E_z/E_P = A_z(E/E_P - 1)$, Eq. 52 for $A_z^{(\infty)}$, and our empirical estimate of $\lim(E/E_P) |_{Ri \rightarrow \infty} = 8$ (resulted form Eq. 59 and Fig. 7) yield:

$$C_\theta = \frac{C_r(1 - 2C_0)(1 - R_\infty) - 3R_\infty}{[1 + (C_P - 1)R_\infty][3 + C_r(1 - 2C_0)]} = 0.105. \tag{64}$$

The above theoretical results are quite unusual considering that the stability dependencies of the dimensionless parameters of turbulence, in particular, the Ri dependencies of the flux Richardson number Ri_f and the turbulent Prandtl number Pr_T , given by Eq. 56, are determined from an unclosed system of equations, regardless of the particular formulation of the turbulent dissipation time scale t_T . The latter is determined in the next section from asymptotic analysis of the velocity shear and TKE budget in the strong- and weak-turbulence regimes.

3.4 Turbulent Dissipation Time and Length Scales

The time scale t_T or the length scale l appear in the Kolmogorov closure for the dissipation rates, Eqs. 1, 19, 25, 33. Until the present, determination of these scales remained one of the most uncertain aspects of the turbulence closure problem. The only simple case, when l is easily determined, is the non-rotating neutrally stratified boundary layer flow over a flat surface, where the turbulent length scale is restricted only by the distance from the surface, z . Then the “master length scale” $l_0 = l|_{Ri=0}$ can be taken proportional to z :

$$l_0 = l|_{Ri=0} = C_l z, \tag{65}$$

where $C_l = \text{constant}$.¹ In stable stratification, an additional restriction appears due to the balance between the kinetic energy of a fluid parcel and its potential energy acquired at the expense of displacement. Using the Obukhov length scale L , Eq. 41, to quantify this restriction, and leaving aside the restriction caused by the Earth’s rotation, it stands to reason that the turbulent length scale l in the stably stratified boundary layer close to the surface monotonically increases with increasing height: $l = l_0 \sim z$ at $z \ll L$, whereas far from the surface it levels off: $l \sim L$ at $z \gg L$.

In view of these two limits, the easiest way to determine l that comes to mind is the interpolation of the type $l \sim z/(1 + \text{constant } z/L)$, employing either the Obukhov length scale L or alternative stratification length scales: $E_K^{1/2}/N$, $\varepsilon_K^{1/2}/N^{3/2}$, etc. However, no such interpolation has led to satisfactory results. The problem is aggravated by the lack of high-quality data on the stability dependence of t_T or l . The point is that $t_T \equiv E_K/\varepsilon_K$ or $l \equiv E_K^{1/2} t_T$ are virtual parameters determined through E_K and ε_K , which both are not easily measurable. Therefore hypothetical interpolation formulae for t_T or l are verified indirectly, through the overall performance of the turbulence closure model. This method does not offer a clear understanding as to which elements of the closure are correct and which are erroneous.

¹ Obukhov (1942) developed a method for determining the master length scale for complex domains.

Instead, Zilitinkevich et al. (2010) have revealed the stability dependence of the turbulent time scale indirectly from the stability dependence of the velocity shear S determined quite accurately in numerous field experiments and LES. For the neutrally stratified boundary-layer flow (with $Ri \ll 1$, $z/L \ll 1$), taking $l = C_l z$ and combining the steady-state version of Eq. 24 with Eqs. 51 and 60 yields the familiar wall law:

$$S = \frac{\tau^{1/2}}{kz}, \tag{66}$$

where k is the von Karman constant expressed through C_l and other dimensionless constants of the EFB closure:

$$k = C_l \left[\frac{2C_\tau C_r}{3(1 + C_r)} \right]^{3/4}. \tag{67}$$

Adopting the conventional empirical value of $k = 0.4$, yields $C_l = 2.66$, and hereafter we include k instead of C_l in the set of basic empirical constants of the EFB closure.

Alternatively, in very stable stratification (at $Ri > 1$, $z/L \gg 1$), Eqs. 39 and 46 yield the following asymptotic expression of the velocity shear:

$$S = \frac{-\beta F_z}{R_\infty \tau} = \frac{\tau^{1/2}}{R_\infty L}. \tag{68}$$

while straightforward interpolation between Eqs. 66 and 68 reads

$$S = \frac{\tau^{1/2}}{kz} \left(1 + \frac{k}{R_\infty} \frac{z}{L} \right). \tag{69}$$

Clearly, there are no a priori grounds to expect that Eq. 69 is valid between the limits set by Eqs. 66 and 68. But fortunately this happens to be the case: Eq. 69 shows excellent agreement with experimental data for steady-state non-rotating sheared flows over the *entire range of stratifications from neutral to extremely stable*.

Indeed, the linear z/L dependence of the “velocity Φ -function”:

$$\Phi_M \equiv \frac{kz}{\tau^{1/2}} S = 1 + C_u \frac{z}{L}, \tag{70}$$

established by Monin and Obukhov (1954) for the stably stratified atmospheric surface layer (where Ri varies from 0 to 0.25, and z/L varies from 0 to 10), was confirmed in numerous experiments (e.g., Monin and Yaglom 1971) and LES that yielded quite solid estimates of the empirical constants $k \approx 0.4$, $C_u \approx 1.6$ (see Fig. 10). On the other hand, adopting the conventional empirical value of $k \approx 0.4$ and the estimate of $R_\infty \approx 0.25$ based on experimental, LES and DNS data for very stably stratified flows (covering a wide range of Ri from 1 to 10^2), the empirical constant k/R_∞ on the r.h.s. of Eq. 69 (precisely analogous to C_u in Eq. 70) is also estimated as $k/R_\infty \approx 1.6$. What this means is that Eq. 69 agrees very well with experimental data on the velocity gradient over the entire range of stratifications from $Ri < 0.25$ (in the atmospheric surface layer) up to $Ri \sim 10^2$ (in LES, DNS and laboratory experiments). On these grounds Eq. 69 can be considered as a firmly established feature of the locally balanced steady-state stably stratified sheared flows.

Combining Eq. 69 with the definition of the flux Richardson number, Eq. 40, yields the following relations linking Ri_f and z/L :

$$Ri_f = \frac{kz/L}{1 + kR_\infty^{-1}z/L}, \quad \frac{z}{L} = \frac{R_\infty}{k} \frac{Ri_f}{R_\infty - Ri_f}. \tag{71}$$

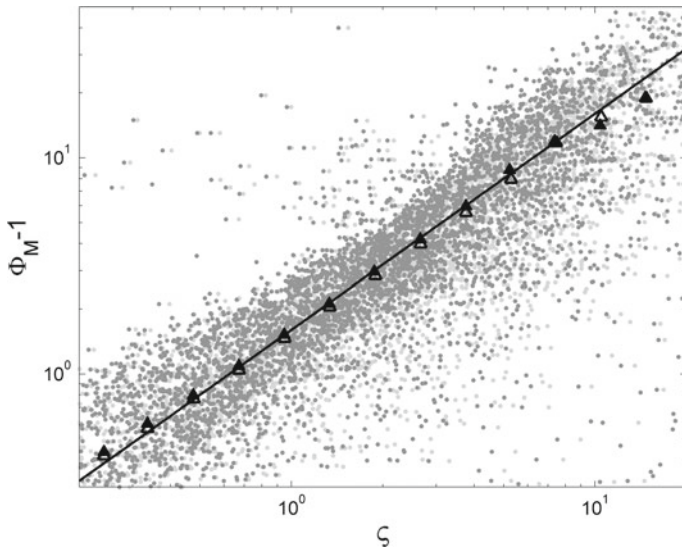


Fig. 10 Dimensionless wind-velocity gradient $\Phi_M = (kz/\tau^{1/2})(\partial U/\partial z)$ versus dimensionless height ζ based on the Obukhov length L in the stably stratified atmospheric boundary layer, after LES (our DATA-BASE64). Solid line is plotted after Eq. 70 with $C_u = k/R_\infty = 1.6$. Open triangles correspond to $\zeta = z/L$, black triangles to $\zeta = z/[1 + C_\Omega \Omega z/E_K^{1/2}]L$ with $C_\Omega = 1$

Furthermore, substituting $-\tau_{i3}\partial U_i/\partial z = \tau S$ after Eq. 69 into the steady-state version of the TKE budget equation, Eq. 24, and accounting for Eq. 71, yields the stability dependence of the turbulent dissipation time and length scales, t_T and l , in terms of either z/L or Ri_f :

$$l = t_T E_K^{1/2} = kz \frac{(E_K/\tau)^{3/2}}{1 + k(R_\infty^{-1} - 1)z/L} = kz \left(\frac{E_K}{\tau}\right)^{3/2} \frac{1 - Ri_f/R_\infty}{1 - Ri_f}, \tag{72}$$

where E_K/τ is expressed by Eq. 60 as a universal function of Ri_f (that can be converted into a function of z/L using Eq. 71). Equation 72 has quite expected asymptotes: $l \sim z$ for $z/L \rightarrow 0$, and $l \sim L$ for $z/L \rightarrow \infty$. However, it essentially differs from the mere linear interpolation between $1/z$ and $1/L$, since the factor $(E_K/\tau)^{3/2}$ on the r.h.s. of Eq. 72 strongly increases with increasing stability and approaches a finite limit only at $Ri > 1$, which is outside geophysical boundary-layer flows, where Ri is typically less than 0.25 (see the empirical Ri dependence of E_K/τ in Fig. 8).

In addition to the effect of stratification, l and t_T are affected by the angular velocity of the Earth's rotation $\Omega = 7.29 \times 10^{-5} \text{ s}^{-1}$, which involves the rotational length-scale limit: $E_K^{1/2}/\Omega$. Accordingly, we determine the master length l_0 interpolating between the surface limit, Eq. 65 and the above mentioned rotational limit, which yields $l_0 = C_l z/(1 + C_\Omega \Omega z/E_K^{1/2})$, where C_Ω is empirical dimensionless constant. Then Eq. 72 becomes

$$\begin{aligned} l = t_T E_K^{1/2} &= \frac{kz}{1 + C_\Omega \Omega z/E_K^{1/2}} \left(\frac{(E_K/\tau)^{3/2}}{1 + k(R_\infty^{-1} - 1)z/L} \right), \\ &= \frac{kz}{1 + C_\Omega \Omega z/E_K^{1/2}} \left(\frac{E_K}{\tau} \right)^{3/2} \left(\frac{1 - Ri_f/R_\infty}{1 - Ri_f} \right). \end{aligned} \tag{73}$$

Blackadar (1962) was probably the first who called attention to the effect of the Earth’s rotation on the turbulent length scale. He proposed a relation analogous to Eq. 73 with the only difference being that the rotational turbulent length-scale limit was defined through the ratio U/f , where U is the mean wind velocity (rather than turbulent velocity scale $E_K^{1/2}$) and $f = 2\Omega \sin \varphi$ is the Coriolis parameter (rather than the angular velocity of Earth’s rotation Ω). In our notation Blackadar’s relation becomes $l_0 = C_l z / (1 + C_B f z / U)$, where C_B is an empirical dimensionless coefficient. Relying upon its commonly accepted empirical value $C_B = 1.5 \times 10^3$ (e.g., Sorbjan 2012) and accounting for the typical value of the intensity of turbulence in the free atmosphere $E_K^{1/2} / U \sim 10^{-3}$, yields a rough estimate of our dimensionless constant: $C_\Omega \sim C_B (E_K^{1/2} / U) \sim 1$. We do not strictly follow Blackadar (1962) because $E_K^{1/2}$ is obviously more relevant than U as the turbulent velocity scale, and Ω is more relevant than f as the rotational frequency scale. Indeed, f characterizes exclusively the vertical component of the vector Ω_i ($i = 1, 2, 3$), which affects the horizontal velocity components, whereas turbulent motions are essentially three-dimensional and are affected by all three components of Ω_i (see Glazunov 2010).

It is significant that the traditional stratification parameters $Ri_f = -\tau S / F_z$ and $z/L = -\beta F_z z / \tau^{3/2}$, widely used in the atmospheric boundary layer, are based on the local values of turbulent fluxes τ and F_z . In the context of the turbulence closure problem, these are just the unknown parameters to be determined. Therefore closure models formulated in terms of Ri_f or z/L imply iteration procedures with no guarantee that errors in determining τ and F_z (in very stable stratification comparable with τ and F_z as such) would not disrupt the convergence of iterations. To overcome this difficulty, we propose a new *energy stratification parameter*:

$$\Pi = E_P / E_K. \tag{74}$$

The steady-state versions of Eqs. 24 and 30 allow us to express Ri_f through Π and vice versa:

$$Ri_f = \frac{\Pi}{C_P + \Pi}. \tag{75}$$

In terms of Π , Eq. (73) becomes

$$t_{TE} = \frac{l}{E_K^{1/2}} = \frac{kz}{E_K^{1/2} + C_\Omega \Omega z} \left(\frac{E_K}{\tau} \right)^{3/2} \left(1 - \frac{\Pi}{\Pi_\infty} \right). \tag{76}$$

Here, $\Pi_\infty = C_P R_\infty / (1 - R_\infty) = 0.14$ is the maximal value of Π corresponding to extremely stable stratification, and the additional subscript “E” in t_{TE} indicates that Eq. 76 determines the turbulent dissipation time scale t_T in the equilibrium state corresponding to a local balance between the production and the dissipation rates of turbulence. The ratio E_K / τ is determined after Eqs. 60 and 75:

$$\left(\frac{E_K}{\tau} \right)^2 = \frac{C_P}{2C_\tau (C_P + \Pi) A_z}, \tag{77}$$

and the vertical share of TKE A_z , is determined after Eqs. 50c and 75:

$$A_z = \frac{E_z}{E_K} = \frac{\Pi_\infty (C_r - 3\Pi / C_P) (C_P + \Pi) - 2C_r C_0 (C_P + \Pi + \infty) \Pi}{3\Pi_\infty (1 + C_r) (C_P + \Pi) - 2C_r (1 + C_0) (C_P + \Pi_\infty) \Pi}. \tag{78}$$

As evidenced by Eqs. 50c (or 78), A_z monotonically decreases with increasing stability and at $Ri_f \rightarrow R_\infty$ (or $\Pi \rightarrow \Pi_\infty$) tends to a finite positive limit, whereas t_{TE} , Eq. 72 diminishes

to zero. Equations 76–78 close the algebraic version of the EFB closure. Clearly, determining t_{TE} (or l) is fully equivalent to the determining the TKE dissipation rate $\varepsilon = E_K/t_K$.

3.5 Application to Boundary-Layer Turbulence

Equation 71 links the flux Richardson number Ri_f with the dimensionless height $\zeta = z/L$ based on the Obukhov length scale L , Eq. 42. This relation is valid not too far from the surface, namely at $z \ll E_K^{1/2}/\Omega$, where the master length scale l_0 , Eq. 73, reduces to $C_l z$. However, in the upper part of the atmospheric boundary layer the effect of Ω on the master length scale l_0 can be significant. Indeed, the TKE at the upper boundary of the layer becomes very small compared to its near-surface value. Taking $\Omega = 7.29 \times 10^{-5} \text{ s}^{-1}$ and adopting a rough estimate of $E_K^{1/2}|_{z=h} \approx 0.1 \text{ m s}^{-1}$ yields the rotational length scale $E_K^{1/2}/\Omega \sim 10^3 \text{ m}$, which is quite comparable with the typical boundary-layer height $h \sim 5 \times 10^2 \text{ m}$. Anyhow, close to the surface the effect of rotation on l_0 is obviously negligible. Hence, using Eq. 71, the dimensionless parameters of turbulence, presented in Sects. 3.2 and 3.3 as universal functions of Ri_f , can be reformulated as universal functions of $\zeta = z/L$.

The concept of similarity of turbulence in terms of the dimensionless height ζ has been proposed by Monin and Obukhov (1954) for the “surface layer” defined as the lower one tenth of the boundary layer, where the turbulent fluxes of momentum τ , temperature F_z and other scalars, as well as the length scale L , are reasonably accurately approximated by their surface values: $\tau = \tau|_{z=0} \equiv u_*^2$, $F_z = F_z|_{z=0} \equiv F_*$, $L = L|_{z=0} \equiv L_*$. This widely recognised similarity concept was confirmed, particularly for stable stratification, in numerous field and laboratory experiments (see Monin and Yaglom 1971; Sorbjan 1989; Garratt 1992) and more recently through LES and DNS. Nieuwstadt (1984) extended this concept to the entire stable boundary layer employing local z -dependent values of the fluxes τ , F_z and the length L instead of their surface values: u_*^2 , F_* and L_* .

The EFB closure as applied to steady-state non-rotating boundary-layer flows is fully consistent with the Monin–Obukhov and Nieuwstadt similarity theories. Considering the immense available information on atmospheric boundary-layer turbulence, we present examples of theoretical relationships potentially useful in modelling applications:

the ratio of TPE to TTE, Eq. 54:

$$\frac{E_P}{E} = \frac{C_P R_\infty \zeta}{R_\infty/k + [1 + (C_P - 1)R_\infty] \zeta}, \tag{79}$$

the vertical share of TKE, Eq. 50c:

$$A_z = \frac{E_z}{E_K} = \frac{R_\infty C_r + k \zeta \left[C_r(1 - 2C_0) - \frac{3R_\infty(R_\infty + k\zeta)}{R_\infty + k\zeta(1 - R_\infty)} \right]}{3R_\infty(1 + C_r) + k\zeta[3 + C_r(1 - 2C_0)]}, \tag{80}$$

the turbulent Prandtl number, Eq. 56:

$$Pr_T = \frac{C_\tau}{C_F} \left[1 + \frac{a_1 \zeta + a_2 \zeta^2}{1 + a_3 \zeta} \right], \tag{81}$$

and the gradient Richardson number [from Eqs. 71, 81]:

$$Ri = Ri_f Pr_T = \frac{C_\tau k \zeta}{C_F(1 + R_\infty^{-1} k \zeta)} \left[1 + \frac{a_1 \zeta + a_2 \zeta^2}{1 + a_3 \zeta} \right], \tag{82}$$

where a_1 , a_2 and a_3 are known empirical constants:

$$a_1 = 3k(1 + C_\tau) \frac{(1 - 2C_0)(R_\infty^{-1} - 1) - 3C_\tau^{-1}}{3 + C_\tau(1 - 2C_0)}, \tag{83}$$

$$a_2 = \frac{k^2}{R_\infty} [(1 - 2C_0)(R_\infty^{-1} - 1) - 3C_\tau^{-1}], \tag{84}$$

$$a_3 = \frac{k}{R_\infty} \left(\frac{6(C_0 + 1)}{3 + C_\tau(1 - 2C_0)} + 2(R_\infty - C_0) - 1 \right). \tag{85}$$

According to the EFB closure, the mean velocity gradient in a steady-state non-rotating boundary-layer flow is expressed by Eq. 69 that implies the following ζ -dependence of the eddy viscosity: $K_M = \tau/S = k\tau^{1/2}z [1 + (k/R_\infty)\zeta]^{-1}$. Therefore Eqs. 71 and 82 allow us to determine the turbulent Prandtl number Pr_T , eddy conductivity $K_H = K_M/Pr_T$, potential temperature gradient $\partial\Theta/\partial z = -F_z/K_H$, and the “temperature Φ -function”:

$$\Phi_H \equiv \frac{k_T \tau^{1/2} z}{-F_z} \frac{\partial\Theta}{\partial z} = \left[1 + \frac{a_1 \zeta + a_2 \zeta^2}{1 + a_3 \zeta} \right] \left(1 + \frac{k}{R_\infty} \zeta \right), \tag{86}$$

where $k_T = (C_F/C_\tau)k = 0.5$ is the temperature von Karman constant, and $k = 0.4$ is the velocity von Karman constant, Eq. 67.

In Fig. 11, Eq. 86 is compared with our LES. Because all model constants in Eq. 86 are already determined from other empirical dependencies, very good agreement between the theory and LES data in Fig. 11 serves as an independent verification of the EFB model. Given the velocity and temperature Φ functions, Eqs. 70 and 86, the ζ dependence of the gradient Richardson number is immediately determined: $Ri = k(C_\tau/C_F)\zeta\Phi_H/\Phi_M^2$. Its comparison with our LES is shown in Fig. 12. Besides the LES data points, in Figs. 10, 11 and 12 we demonstrate the two versions of the bin-averaged data shown as open triangles for $\zeta = z/L$ and black triangles for $\zeta = z/((1 + C_\Omega\Omega z/E_K^{1/2})L)$ with $C_\Omega = 1$. In Figs. 11 and 12 black triangles obviously better fit theoretical curves at large ζ . This supports the estimate of $C_\Omega = 1$ and confirms that the Earth’s rotation starts affecting the turbulent length and time scales already in the upper part of the planetary boundary layer—at a few hundred m height.

To the best of our knowledge, none of Eqs. 79–86 has been obtained before. Moreover, in the traditional interpretation of the Monin–Obukhov similarity theory it was taken as self-evident that the maximal values of $\zeta = z/L$ achievable in the atmospheric surface layer (factually never exceeding 10) can be attributed to the very strong static stability regime that was given the name “z-less stratification regime”. Accordingly, it was assumed that at $z \gg L$ the distance above the surface does not affect turbulence and, therefore, should disappear from any similarity-theory relations, for instance, from the expressions on the r.h.s. of Eqs. 79–81, 85, which therefore should turn into universal constants.

This reasoning is not quite correct, since the point is that really strongly-stable stratification is principally unattainable neither in the surface layer nor in the atmospheric boundary layer. The boundary-layer flows correspond to quite small gradient Richardson numbers $Ri \ll 1$ and only moderate dimensionless heights $\zeta \ll 10$. Moreover, even at $\zeta \rightarrow \infty$, the similarity functions do not necessarily turn into finite constants, but can also tend to zero (as for instance the dimensionless heat flux: Eq. 61 and Fig. 9) or to infinity (as, for instance, the ζ dependencies of Ri and Pr_T : Eq. 82 and Fig. 5). Factually, the atmospheric boundary layer is a *weakly-stable* strong-turbulence layer characterized by the gradient Richardson number essentially < 1 and dimensionless heights $\zeta = z/L < 10$. The *strongly-stable* stratification with $Ri \gg 1$ and $\zeta \gg 10^2$ corresponds to the weak-turbulence regime typical of the free atmosphere.

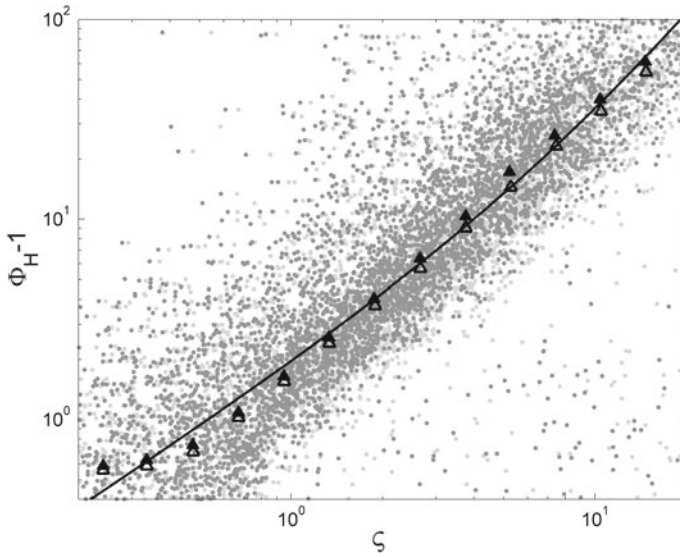


Fig. 11 Same as in Fig. 10 but for the dimensionless potential temperature gradient $\Phi_H = (-k_T z \tau^{1/2} / F_z) (\partial \Theta / \partial z)$. Solid line is plotted after Eq. 86. Open triangles correspond to $\zeta = z/L$, black triangles to $\zeta = z/[(1 + C_\Omega \Omega z / E_K^{1/2})L]$

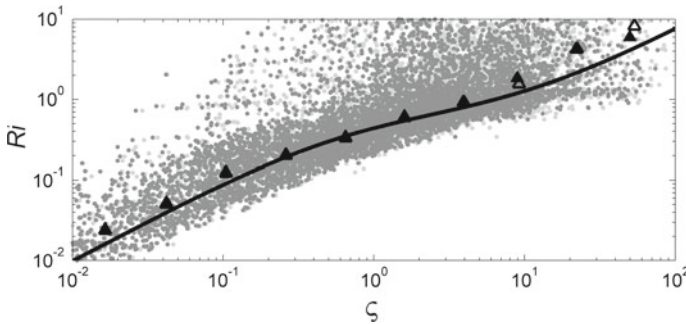


Fig. 12 Gradient Richardson number Ri versus dimensionless parameters $\zeta = z/L$ (white triangles) and $\zeta = l_0/L$ (black triangles) based on the Obukhov length scale L , after our LES. Solid line shows our model. Open triangles correspond to $\zeta = z/L$, black triangles to $\zeta = z/[(1 + C_\Omega \Omega z / E_K^{1/2})L]$

4 Hierarchy of EFB Turbulence Closures

4.1 General Prognostic Model

The algebraic model presented in Sect. 3 is based on the steady-state versions of the energy- and flux-budget equations, Eqs. 24, 30, 34, 37; and, as with any other algebraic closure, has a limited area of application (in particular, it erroneously prescribes total decay of turbulence in the regions of flow with zero mean shear, e.g., at the axes of jets). In its general form, the EFB closure employs prognostic versions of the above equations, with the non-local third-order transport terms Φ_K , Φ_P , $\Phi_i^{(\tau)}$ and $\Phi_z^{(F)}$ expressed through the conventional turbulent diffusion approximation:

$$\frac{DE_K}{Dt} - \frac{\partial}{\partial z} K_E \frac{\partial E_K}{\partial z} = -\tau_{i3} \frac{\partial U_i}{\partial z} + \beta F_z - \frac{E_K}{t_T}, \tag{87}$$

$$\frac{DE_P}{Dt} - \frac{\partial}{\partial z} K_E \frac{\partial E_P}{\partial z} = -\beta F_z - \frac{E_P}{C_P t_T}, \tag{88}$$

$$\frac{D\tau_{i3}}{Dt} - \frac{\partial}{\partial z} K_{FM} \frac{\partial \tau_{i3}}{\partial z} = -2E_z \frac{\partial U_i}{\partial z} - \frac{\tau_{i3}}{C_\tau t_T} \quad (i = 1, 2), \tag{89}$$

$$\frac{DF_z}{Dt} - \frac{\partial}{\partial z} K_{FH} \frac{\partial F_z}{\partial z} = -2(E_z - C_\theta E_P) \frac{\partial \Theta}{\partial z} - \frac{F_z}{C_F t_T}. \tag{90}$$

The turbulent transport coefficients: K_E for the turbulent energies, and K_{FM} , K_{FH} for the turbulent fluxes are taken proportional to the eddy viscosity K_M , Eq. 43:

$$K_E/C_E = K_{FM}/C_{FM} = K_{FH}/C_{FH} = E_z t_T, \tag{91}$$

where C_E , C_{FM} and C_{FH} are dimensionless constants to be determined empirically.

Generally speaking, the vertical component of TKE E_z is governed by the prognostic Eq. 21 with the pressure terms Q_{ii} determined through the inter-component energy exchange concept, Eqs. 48–49. For practical purposes we recommend a simpler approach based on the quite natural assumption that the TKE components are transported altogether. Then, given E_K , the vertical TKE (which appears in Eqs. 89, 90) is determined as $E_z = A_z E_K$, where $A_z = A_z(\Pi)$ is determined by Eq. 78 with $\Pi = E_P/E_K$ based on the prognostic parameters E_K and E_P :

$$E_z = A_z E_K, \quad A_z = A_z(\Pi) \text{ [Eq. 78]}, \quad \Pi = \frac{E_P \text{ [Eq. 88]}}{E_K \text{ [Eq. 87]}}. \tag{92}$$

We recall that the TKE E_K and its dissipation rate ε_K vary in space and time and are transported by both the mean flow and the turbulence. Hence, the turbulent dissipation time scale $t_T = E_K/\varepsilon_K$ is also transported in space and varies in time. In the steady state, its local-equilibrium value t_{TE} is expressed through E_K , A_z and Π by Eqs. 76–78. Generally the equilibrium is, on the one hand, distorted due to non-steady and non-local processes and, on the other hand, re-established by the local adjustment mechanisms. Such counteractions are modelled by the relaxation equation:

$$\frac{Dt_T}{Dt} - \frac{\partial}{\partial z} K_T \frac{\partial t_T}{\partial z} = -C_R \left(\frac{t_T}{t_{TE}} - 1 \right), \quad t_{TE} = t_{TE}(E_K, A_z, \Pi) \text{ [Eqs. 76–78]}, \tag{93}$$

where the relaxation time is taken proportional to the local-equilibrium dissipation time scale t_{TE} determined through E_K , A_z and Π by Eq. 76–78; $K_T = C_T E_z t_T$ is the same kind of turbulent exchange coefficient as K_E , K_{FM} , K_{FH} ; C_T and C_R are dimensionless constants to be determined empirically.

By and large, the general EFB closure model consists of:

- (a) five prognostic Eqs. 87–90, 93 for TKE E_K , TPE E_P , vertical turbulent flux of momentum τ_{i3} ($i = 1, 2$), vertical turbulent flux of potential temperature F_z , and turbulent dissipation time scale t_T (which determines the TKE dissipation rate $\varepsilon_K = E_K/t_T$);
- (b) three diagnostic relations: Eq. 76 for the local-equilibrium turbulent time scale t_{TE} , Eq. 77 for E_K/τ , and Eq. 78 for the vertical share of TKE A_z .

In addition to empirical constants of the algebraic version of the EFB closure (already determined in Sect. 3), the general EFB closure includes additional constants C_E , C_{FM} , C_{FH} , C_T and C_R that are to be determined through case studies by fitting results from numerical modelling with observational and LES data.

Compared to the currently used closure models, the EFB closure benefits from the following advancements:

- consistent energetics based on the prognostic budget equations for TKE E_K and TPE E_P , Eq. 87 and 88, and reliable stratification parameter $\Pi = E_P/E_K$;
- generally non-gradient concept of the turbulent transport based on the budget equations for the turbulent fluxes, Eqs. 89–90;
- advanced concept of the inter-component exchange of TKE, Eqs. 48–50, 78;
- advanced concept of the turbulent dissipation time scale, Eqs. 76, 93.

4.2 Down-Gradient Transport Models

In a number of problems the steady-state version of the flux-budget Eqs. 89–90 provides a quite sufficient approximation. It essentially simplifies the model, keeping in force all the above benefits, except for the possibility of reproducing presumably rare cases of the non-gradient turbulent transports. Therefore, for extensive environmental-modelling applications, the EFB closure can be reduced to the following equations:

- Prognostic energy budget equations, Eqs. 87 and 88, for TKE E_K and TPE E_P , supplemented with diagnostic formulation, Eq. 92, for the vertical TKE E_z ;
- Prognostic formulation, Eqs. 76–78, 93, for the turbulent dissipation time scale t_T ;
- Steady-state versions of the flux-budget equations, Eqs. 89 and 90, that provide diagnostic down-gradient transport formulation of the vertical turbulent fluxes in terms of the eddy viscosity K_M and eddy conductivity K_H :

$$\tau_{i3} = -K_M \frac{\partial U_i}{\partial z}, \quad F_z = -K_H \frac{\partial \Theta}{\partial z}, \tag{94}$$

$$K_M = 2C_\tau E_z t_T, \quad K_H = 2C_F E_z t_T \left(1 - C_\theta \frac{E_P}{E_z} \right), \tag{95}$$

where E_z , E_P and t_T are determined through the equations listed above in paragraphs (a) and (b). As needed, the model can be further simplified keeping only two prognostic equations, Eqs. 87 and 88, for E_K and E_P ; and determining other parameters diagnostically: E_z —through Eq. 92, $t_T = t_{TE}$ —through Eqs. 76–78, and the vertical turbulent fluxes τ_{i3} and F_z —through Eqs. 94 and 95.

4.3 Minimal Prognostic Model

Until recently common practice was limited to the sole use of the TKE budget equation—e.g. Mauritsen et al. (2007) and Angevine et al. (2010) employed the TTE budget equation. Be that as it may, closure models based on only one prognostic energy budget equation inevitably miss some essential features of non-steady regimes of turbulence. Principal inaccuracy of the one-equation approach is rooted in the difference between the TPE and TKE dissipation times: $C_P t_T$ and t_T , respectively. Because $C_P = 0.86$ (see Sect. 3.3), TPE dissipates more rapidly than TKE, which is why one particular equation (for TKE, TPE or TTE) is insufficient to accurately reproducing turbulence energetics. With this warning, we propose the simplest prognostic version of the EFB closure model based on the TTE budget equation:

$$\frac{DE}{Dt} - \frac{\partial}{\partial z} K_E \frac{\partial E}{\partial z} = -\tau_{i3} \frac{\partial U_i}{\partial z} - \frac{E}{t_T [1 - (1 - C_P) Ri_f]} \tag{96}$$

It is derived by adding Eqs. 87 and 88 and expressing the sum $E_K + E_P/C_P$ approximately through diagnostic Eqs. 53 and 54. Equation 96 is preferable compared to the TKE budget equation because E is a conserved property (it becomes an invariant in the absence of production and dissipation) in contrast to E_K that continuously feeds the potential energy E_P . Except for E , all other parameters are determined in this version of the closure diagnostically:

(a) E_K, E_P —through Eqs. 53, 54:

$$E_K = E \frac{1 - Ri_f}{1 - (1 - C_P)Ri_f}, \quad E_P = E \frac{C_P Ri_f}{1 - (1 - C_P)Ri_f}, \tag{97}$$

(b) A_z and E_z —through Eq. 50c:

$$A_z = \frac{C_r(1 - 2C_0 Ri_f/R_\infty)(1 - Ri_f) - 3Ri_f}{(1 - Ri_f)\{3 + C_r[3 - 2(1 + C_0)Ri_f/R_\infty]\}}, \quad E_z = A_z E_K, \tag{98}$$

(c) t_T —through Eq. 76 rewritten in terms of Ri_f :

$$t_{TE} = \frac{kz}{E_K^{1/2} + C_\Omega \Omega z} \left(\frac{E_K}{\tau} \right)^{3/2} \frac{1 - Ri_f/R_\infty}{1 - Ri_f}, \tag{99}$$

(d) τ_{i3} and F_z —through Eqs. 43, 44, 97:

$$\tau_{i3} = -K_M \frac{\partial U_i}{\partial z}, \quad K_M = 2C_\tau E_z t_T, \tag{100}$$

$$F_z = -K_H \frac{\partial \Theta}{\partial z}, \quad K_H = 2C_F E_z t_T \left(1 - \frac{C_\theta C_P Ri_f}{(1 - Ri_f)A_z} \right), \tag{101}$$

(e) Ri_f —through its definition, Eq. 39:

$$Ri_f = \frac{-\beta F_z}{\tau_{i3} \partial U_i / \partial z}. \tag{102}$$

Setting the l.h.s. of Eq. 96 equal to zero, this model reduces to the steady-state EFB model considered in detail in Sect. 3.

5 Conclusions

Over several decades, operationally used closure models conceptually followed Kolmogorov (1941, 1942): they limited the representation of turbulence energetics to the TKE budget equation and employed hypothetical expressions of the eddy viscosity and eddy conductivity of the type $K_M \sim K_H \sim E_K t_T \sim E_K^{1/2} l$. This “one energy-equation approach”, originally proposed for neutrally stratified flows (and justified for neutral stratification), became misleading when applied to stably stratified flows. It disregarded the energy exchange between TKE and TPE controlled by the buoyancy flux βF_z and, therefore, disguised the condition that $-\beta F_z$ in the steady state cannot exceed the shear production of TKE. This confusion gave rise to the erroneous but widely believed statement that steady-state turbulence can be maintained by the velocity shear only at small gradient Richardson numbers: $Ri < Ri_c < 1$, whereas at $Ri > Ri_c$ turbulence inevitably degenerates and the flow becomes laminar.

Obukhov (1946) was the first who applied the Kolmogorov closure to the thermally stratified atmospheric surface layer. He accounted for the term βF_z in the TKE equation (which led him to discover the stratification length scale L , Eq. 41, now called the “Obukhov scale”)

but in all other respects he retained the original Kolmogorov closure absolutely unchanged. In particular, he disregarded the role of the TPE and the TKE \leftrightarrow TPE energy exchange. Moreover, Obukhov preserved even the concept of the turbulence length scale l as merely proportional to the height z , precisely as was stated in Kolmogorov (1941, 1942). And that is in spite of Obukhov's own discovery of the length scale L , which gave him grounds to conclude that l should tend to L in strongly stable stratification. It is beyond question that his model, generalizing the logarithmic wall law for the stratified flows, has made a great stride forward in the physics of turbulence, not to mention that eventually it gave rise to the famous surface-layer similarity theory (Monin and Obukhov 1954). However, in the context of turbulence closure problem, Obukhov's model was, to some extent, misleading. It is due to the great authority of Kolmogorov, Obukhov and their school of turbulence, that further efforts towards the development of turbulence closure models for meteorological and oceanographic applications were over half a century limited to "mechanical closures" based on the sole use of the TKE budget equation, disregarding the TPE, and applied for only cautious corrections to Eq. (2): $K_M \sim K_H \sim E_K^{1/2} l_T$. This historical remark explains why a rather simple "mechanical and thermodynamic" EFB turbulence closure was not developed already long ago.

Our work on the EFB closure, commencing with Elperin et al. (2005) and reflected in Zilitinkevich et al. (2007, 2008, 2009, 2010), has been inspired by numerous experimental and numerical modelling studies that disclosed essential features of stably stratified turbulence that dramatically contradicted traditional closure models (e.g. Fig. 5 demonstrating asymptotically a linear Ri dependence of the turbulent Prandtl number). The present paper summarizes results from this work. Compared to previous versions of the EFB closure, we now advance the concept of the inter-component exchange of TKE (Sect. 3.2); clarify the physical meaning of the turbulent dissipation time and length scales and have developed diagnostic and prognostic models for these scales (Sects. 3.4 and 4.1); and have formulated a hierarchy of EFB turbulence closures at different levels of complexity designed for different applications.

The steady-state version of the EFB closure allows us to determine the stability dependencies of the velocity and temperature gradients, the eddy viscosity and eddy conductivity, and many other parameters of turbulence as functions of the dimensionless height z/L (Sect. 3.5). It sheds new light on the Monin and Obukhov (1954) and Nieuwstadt (1984) similarity theories and extends these to a much wider range of stably stratified flows. Eq. 82, linking z/L with the gradient Richardson number Ri , reveals that the notion "strongly stable stratification" is currently used in a rather uncertain sense. In boundary-layer meteorology, it implies nothing but the strongest stratifications achievable in the atmospheric boundary layer, which factually corresponds to the values of z/L in the interval $1 < z/L < 10$. However, as follows from Eq. 82, $z/L < 10$ corresponds to $Ri < 1$, that is to only *weakly-stable* stratification inherent in the strong-turbulence regime. On the contrary, the *strongly-stable* stratification inherent in the weak-turbulence regime is observed only outside the boundary layer, in the free atmosphere, where Ri varies typically from 1 to 10^2 , and could peak at 10^3 in the capping inversions above the long-lived stable boundary layer. The above terminological confusion has led to the erroneous treatment of the so-called z -less stratification regime (associated with maximal z/L achievable in the surface layer) as the ultimate strongly-stable stratification regime. As a result, the similarity theory in its traditional form was incapable of correctly determining the asymptotic behaviour of the similarity functions at very large z/L . Equations 70 and 86 refine traditional surface-layer flux-profile relationships and offer scope for improving the surface-flux algorithms in atmospheric models.

Empirical validation of a turbulence closure model often reduces to comparison with empirical data of the model results related only to the turbulent fluxes (τ , F_z , etc.) and the mean flow parameters (\mathbf{U} , Θ , etc.), with no consideration of other conclusions from the model. Thus, we never found in the literature verifications of the operationally used TKE-budget closure models in terms of the stability dependences of the ratios E_K/τ or $\varepsilon_K/(\tau S)$ in the steady state. In contrast, we verify results from our theory related to all the considered characteristics of turbulence, first of all, in the steady-state regime of turbulence. This work faces essential difficulties because of the lack of data on steady-state turbulence in strongly stable stratification, and we were forced to very carefully select appropriate data presented in our figures. Comprehensive empirical validation of the EFB turbulence closure is yet to be performed. New, specially designed DNS and laboratory experiments are needed to realistically reproduce the weak-turbulence regime in stationary and homogeneous conditions. Alternative validation tools, to provide case studies of the very stably stratified turbulent flows in the atmosphere and hydrosphere, might use numerical models equipped with the EFB turbulence closure employing our tentative estimates of the empirical constants.

We propose different prognostic versions of the EFB closure, from the most general (Sect. 4.1) to the minimal (Sect. 4.3), for use in different applications depending on available computational resources and scientific or operational goals. The general and the down-gradient transport versions of the EFB closure (Sects. 4.1 and 4.2) are recommended for modeling the so-called “optical turbulence”. The latter is controlled by the temperature-fluctuation “energy” $E_\theta = (N/\beta)^2 E_p$ (Lascaux et al. 2009) and, therefore, cannot be reliably recovered from the turbulence closures disregarding the TPE budget equation. For operational numerical weather prediction, air quality and climate modelling, we recommend, as sufficiently accurate and not too computationally expensive, the three-equation version of the TKE closure (Sect. 4.2).

Acknowledgments This work has been supported by the EC FP7 ERC Grant No. 227915 “Atmospheric planetary boundary layers—physics, modelling and role in Earth system”; the Russian Federation Government Grant No. 11.G34.31.0048 “Air-sea/land interaction: physics and observation of planetary boundary layers and quality of environment”; the Israel Science Foundation governed by the Israeli Academy of Sciences, Grants No. 259/07 and No. 1037/11; and the Norwegian Research Council Grant No. 191516/V30 “Planetary Boundary Layer Feedback in the Earth’s Climate System”. Our thanks to Rostislav Kouznetsov (A.M. Obukhov Institute of Atmospheric Physics, Moscow/Finnish Meteorological Institute, Helsinki) for his contribution to Figs. 1, 2, 3 and 6; and to Frank Beyrich (German Weather Service) for providing us with the Lindenberg data shown in Fig. 6.

References

- Angevine WM, Jiang H, Mauritsen T (2010) Performance of an eddy diffusivity–mass flux scheme for shallow cumulus boundary layers. *Mon Weather Rev* 138:2895–2912
- Banta RM, Newsom RK, Lundquist JK, Pichugina YL, Coulter RL, Mahrt L (2002) Nocturnal low-level jet characteristics over Kansas during CASES-99. *Boundary-Layer Meteorol* 105:221–252
- Bertin F, Barat J, Wilson R (1997) Energy dissipation rates, eddy diffusivity, and the Prandtl number: an in situ experimental approach and its consequences on radar estimate of turbulent parameters. *Radio Sci* 32:791–804
- Blackadar AK (1962) The vertical distribution of wind and turbulent exchange in a neutral atmosphere. *J Geophys Res* 67:3095–3102
- Canuto VM (2002) Critical Richardson numbers and gravity waves. *Astron Astrophys* 384:1119–1123
- Canuto VM (2009) Turbulence in astrophysical and geophysical flows. *Lect Notes Phys* 756:107–160
- Canuto VM, Howard A, Cheng Y, Dubovikov MS (2001) Ocean turbulence. Part I: one-point closure model—momentum and heat vertical diffusivities. *J. Phys. Oceanogr.* 31:1413–1426

- Canuto VM, Cheng Y, Howard AM (2005) What causes the divergences in local second-order closure models?. *J Atmos Sci* 62:1645–1651
- Canuto VM, Cheng Y, Howard AM, Esau IN (2008) Stably stratified flows: a model with no $Ri(cr)$. *J Atmos Sci* 65:2437–2447
- Cheng Y, Canuto VM, Howard AM (2002) An improved model for the turbulent PBL. *J Atmos Sci* 59:1550–1565
- Churchill SW (2002) A reinterpretation of the turbulent Prandtl number. *Ind Eng Chem Res* 41:6393–6401
- Elperin T, Kleeorin N, Rogachevskii I (1996) Isotropic and anisotropic spectra of passive scalar fluctuations in turbulent fluid flow. *Phys Rev E* 53:3431–3441
- Elperin T, Kleeorin N, Rogachevskii I, Zilitinkevich S (2002) Formation of large-scale semi-organized structures in turbulent convection. *Phys Rev E* 66(066305):1–15
- Elperin T, Kleeorin N, Rogachevskii I, Zilitinkevich S (2005) New turbulence closure equations for stable boundary layer. Return to Kolmogorov (1941). In: 5th annual meeting of the European Meteorological Society, Utrecht, The Netherlands, September 12–16, 2005, paper No. 0553
- Elperin T, Kleeorin N, Rogachevskii I, Zilitinkevich S (2006) Turbulence and coherent structures in geophysical convection. *Boundary-Layer Meteorol* 119:449–472
- Engelbart DAM, Andersson S, Görsdorf U, Petenko IV (2000) The Lindenberg SODAR/RASS experiment LINEX-2000: concept and first results. In: Proceedings of 10th international symposium Acoustic Remote Sensing, Auckland, New Zealand, pp 270–273
- Esau I (2004) Simulation of Ekman boundary layers by large eddy model with dynamic mixed sub-filter closure. *Environ Fluid Mech* 4:273–303
- Esau I (2009) Large-eddy simulations of geophysical turbulent flows with applications to planetary boundary layer research, arXiv:0907.0103v1. DATABASE64 could be found on <ftp://ftp.nersc.no/igor/NEW%20DATABASE64/>
- Esau IN, Zilitinkevich SS (2006) Universal dependences between turbulent and mean flow parameters in stably and neutrally stratified planetary boundary layers. *Nonlin Process Geophys* 13:135–144
- Foken T (2006) 50 years of the Monin–Obukhov similarity theory. *Boundary-Layer Meteorol* 119:431–447
- Garratt JR (1992) The atmospheric boundary layer. Cambridge University Press, U.K., 316 pp
- Glazunov AV (2010) On the effect that the direction of geostrophic wind has on turbulence and quasi-ordered large-eddy structures in the atmospheric boundary layer. *Izvestiya RAN, FAO* 46:786–807
- Holton JR (2004) An introduction to dynamic meteorology. Academic Press, New York, 535 pp
- Itsweire EC, Helland KN, Van Atta CW (1986) The evolution of grid-generated turbulence in a stably stratified fluid. *J Fluid Mech* 162:299–338
- Kaimal JC, Finnigan JJ (1994) Atmospheric boundary layer flows. Oxford University Press, New York, 289 pp
- Kraus EB, Businger JA (1994) Atmosphere–ocean interaction. Oxford University Press, Oxford and New York, 362 pp
- Kolmogorov AN (1941) Energy dissipation in locally isotropic turbulence. *Doklady AN SSSR* 32(1):19–21
- Kolmogorov AN (1942) Equations of turbulent motion in an incompressible fluid. *Izv AN SSSR Ser Fiz* 6(1–2):56–58
- Kondo J, Kanechika O, Yasuda N (1978) Heat and momentum transfer under strong stability in the atmospheric surface layer. *J Atmos Sci* 35:1012–1021
- Kurbatsky AF (2000) Lectures on turbulence. Novosibirsk State University Press, Novosibirsk
- Kurbatsky AF, Kurbatskaya LI (2006) Three-parameter model of turbulence for the atmospheric boundary layer over an urbanized surface. *Izvestiya RAN, FAO* 42:439–455
- Kurbatsky AF, Kurbatskaya LI (2009) $E - \varepsilon - \left(\theta^2\right)$ turbulence closure model for an atmospheric boundary layer including the urban canopy. *Meteorol Atmos Phys* 104:63–81
- Kurbatsky AF, Kurbatskaya LI (2010) On the turbulent Prandtl number in a stably stratified atmospheric boundary layer. *Izvestiya RAN, FAO* 40:169–177
- Lascaux F, Masciardi E, Hagelin S, Stoesz J (2009) Mesoscale optical turbulence simulations at Dome C. I: surface layer thickness and seeing in the free atmosphere. *MNRAS* 398(849):193
- Lorenz EN (1955) Available potential energy and the maintenance of the general circulation. *Tellus* 7:157–167
- Lumley JL, Panofsky HA (1964) The structure of atmospheric turbulence. Interscience, New York, 239 pp
- L'vov VS, Procaccia I, Rudenko O (2008) Turbulent fluxes in stably stratified boundary layers. *Phys Scr T132(014010):1–15*
- L'vov VS, Procaccia I, Rudenko O (2009) Energy conservation and second-order statistics in stably stratified turbulent boundary layers. *Environ Fluid Mech* 9:267–295
- Mahrt L, Vickers D (2005) Boundary layer adjustment over small-scale changes of surface heat flux. *Boundary-Layer Meteorol* 116:313–330

- Mauritsen T, Svensson G, Zilitinkevich SS, Esau I, Enger L, Grisogono B (2007) A total turbulent energy closure model for neutrally and stably stratified atmospheric boundary layers. *J Atmos Sci* 64:4117–4130
- Mellor GL, Yamada T (1974) A hierarchy of turbulence closure models for planetary boundary layers. *J Atmos Sci* 31:1791–1806
- Monin AS, Obukhov AM (1954) Main characteristics of the turbulent mixing in the atmospheric surface layer. *Trudy Geophys Inst AN SSSR* 24(151):153–187
- Monin AS, Yaglom AM (1971) *Statistical fluid mechanics*, vol 1. MIT Press, Cambridge
- Mydlarski L (2003) Mixed velocity-passive scalar statistics in high-Reynolds-number turbulence. *J. Fluid Mech.* 475:173–203
- Nieuwstadt FTM (1984) The turbulent structure of the stable, nocturnal boundary layer. *J Atmos Sci* 41:2202–2216
- Obukhov AM (1942) On the shape of the turbulent length scale in flows with arbitrary geometry. Institute of Mechanics USSR Academy of Sciences. *Appl Math Mech* 6:209–220
- Obukhov AM (1946) Turbulence in thermally inhomogeneous atmosphere. *Trudy In-ta Teoret Geofiz AN SSSR* 1:95–115
- Ohya Y (2001) Wind-tunnel study of atmospheric stable boundary layers over a rough surface. *Boundary-Layer Meteorol* 98:57–82
- Ostrovsky LA, Troitskaya Yul (1987) A model of turbulent transfer and dynamics of turbulence in a stratified shear flow. *Izvestiya AN SSSR FAO* 23:1031–1040
- Poulos GS, Blumen W, Fritts DC, Lundquist JK, Sun J, Burns SP, Nappo C, Banta R, Newsom R, Cuxart J, Terradellas E, Balsley B, Jensen M (2002) CASES-99: a comprehensive investigation of the stable nocturnal boundary layer. *Bull Am Meteorol Soc* 83:555–581
- Rehmann CR, Koseff JR (2004) Mean potential energy change in stratified grid turbulence. *Dyn Atmos Oceans* 37:271–294
- Richardson LF (1920) The supply of energy from and to atmospheric eddies. *Proc R Soc Lond A* 97:354–373
- Rogers MM, Mansour NN, Reynolds WC (1989) An algebraic model for the turbulent flux of a passive scalar. *J Fluid Mech* 203:77–101
- Rotta JC (1951) Statistische theorie nichthomogener turbulenz. *Z Physik* 129:547–572
- Schumann U, Gerz T (1995) Turbulent mixing in stably stratified shear flows. *J Appl Meteorol* 34:33–48
- Shih LH, Koseff JR, Ferziger JH, Rehmann CR (2000) Scaling and parameterisation of stratified homogeneous turbulent shear flow. *J Fluid Mech* 412:1–20
- Sorbjan Z (1989) Structure of the atmospheric boundary layer. Prentice-Hall, Englewood Cliffs, 317 pp
- Sorbjan Z (2012) A study of the stable boundary layer based on a single-column K-theory model. *Boundary-Layer Meteorol* 142:33–53
- Srivat A, Warhaft Z (1983) The effect of a passive cross-stream temperature gradient on the evolution of temperature variance and the heat flux in grid turbulence. *J Fluid Mech* 128:323–346
- Strang EJ, Fernando HJS (2001) Vertical mixing and transports through a stratified shear layer. *J Phys Oceanogr* 31:2026–2048
- Stretch DD, Rottman JW, Nomura KK, Venayagamoorthy SK (2001) Transient mixing events in stably stratified turbulence. In: 14th Australasian fluid mechanics conference, Adelaide, Australia, 10–14 December 2001
- Sukoriansky S, Galperin B (2008) Anisotropic turbulence and internal waves in stably stratified flows (QNSE theory). *Phys Scr T132(014036)*:1–8
- Tennekes H, Lumley JL (1972) *A first course in turbulence*. The MIT Press, Cambridge/London, 300 pp
- Uttal T, Curry JA, McPhee MG, Perovich DK, 24 other co-authors (2002) Surface heat budget of the Arctic Ocean. *Bull Am Meteorol Soc* 83:255–276
- Venayagamoorthy SK, Stretch DD (2006) Lagrangian mixing in decaying stably stratified turbulence. *J Fluid Mech* 564:197–226
- Venayagamoorthy SV, Stretch DD (2010) On the turbulent Prandtl number inhomogeneous stably stratified turbulence. *J Fluid Mech* 644:359–369
- Yoon KH, Warhaft Z (1990) The evolution of grid-generated turbulence under conditions of stable thermal stratification. *J Fluid Mech* 215:601–638
- Zilitinkevich SS (2010) Comments on numerical simulation of homogeneous stably stratified turbulence. *Boundary-Layer Meteorol* 136:161–164
- Zilitinkevich SS, Elperin T, Kleerorin N, Rogachevskii I (2007) Energy- and flux-budget (EFB) turbulence closure model for the stably stratified flows. Part I: steady-state, homogeneous regimes. *Boundary-Layer Meteorol* 125:167–192
- Zilitinkevich SS, Elperin T, Kleerorin N, Rogachevskii I, Esau I, Mauritsen T, Miles MW (2008) Turbulence energetics in stably stratified geophysical flows: strong and weak mixing regimes. *Q J R Meteorol Soc* 134:793–799

- Zilitinkevich SS, Elperin T, Kleeorin N, L'vov V, Rogachevskii I (2009) Energy- and flux-budget (EFB) turbulence closure model for stably stratified flows. Part II: the role of internal gravity waves. *Boundary-Layer Meteorol* 133:139–164
- Zilitinkevich SS, Esau I, Kleeorin N, Rogachevskii I, Kouznetsov RD (2010) On the velocity gradient in the stably stratified sheared flows. Part I: asymptotic analysis and applications. *Boundary-Layer Meteorol* 135:505–511